Supplementary Information

Kinetic and Structure-Activity Studies of the Triazolium Ion-catalysed Benzoin Condensation

Richard S. Massey,[a] Jacob Murray [a], Christopher J. Collett,[b] Jiayun Zhu,[a] Andrew D. Smith[b] and AnnMarie C. O'Donoghue[a] *

---

[a] *Department of Chemistry, Durham University, South Road, Durham DH1 3LE, U.K.*

[b] *EaStCHEM, School of Chemistry, University of St. Andrews, North Haugh, St. Andrews KY16 9SY, U.K.*

Contents

S1 Experimental *3*

S1.1 Instrumentation **3**

S1.2 Materials **3**

S1.3 Syntheses **3**

S2 Initial Rate Kinetic Measurements Under Catalytic Conditions *5*

S2.1 Reaction Data and Initial Rate Determination **5**

S 2.1.1. Thiazolium Chloride (**1**) 5

S 2.1.2. Triazolium Tetrafluoroborate **2a** 10

S 2.1.3. Triazolium Tetrafluoroborate **2b** 14

S 2.1.4. Triazolium Tetrafluoroborate **2c** 16

S 2.1.5. Triazolium Tetrafluoroborate **2d** 21

S 2.1.6. Triazolium Tetrafluoroborate **2e** 23

S 2.1.7. Triazolium Tetrafluoroborate **2f** 25

S2.2 Initial Rate Plots versus [PhCHO]$_0$ and Steady State Kinetic Fitting **27**

..... 27

S3 Determination of k_{BI} from Concentration Profiles under Stoichiometric Conditions ... *30*

S4 Steady State Equation Derivation and Validity *32*

S4.1 Derivation of the Steady State Equation **32**

With reference to Scheme 1 in the main manuscript: **32**

S4.2 Validity of the Steady State Fit and Assumption [III]=[I] **33**

S 4.2.1. Half-life Determination for Equilibration of Triazolium Catalysts **2a-d**, Benzaldehyde and Adduct **III** in the Forward Direction 33

S 4.2.2. Berkeley-Madonna Global Fitting – Determination of % Free Catalyst at Equilibrium 33

S 4.2.3. Summary Table 35

S5 Hammett Plot including Data for Triazolium Salt 2f *36*

S6 'Brønsted' Plots *37*

S7 HPLC Chromatograms of Benzoin versus Benzaldehyde *38*

S8 References *39*

S1 Experimental

S1.1 Instrumentation

NMR spectra were collected at 400, 500 and 700 MHz on Varian Mercury-400, Bruker Avance-400, Varian Inova 500 and Varian VNMRS-700 instruments and referenced to deuterated solvent peaks.[S1] Low resolution mass spectrometry was performed on a Waters TQD mass spectrometer. High resolution mass spectrometry was performed on a Thermo-Finnigan LTQ FT mass spectrometer. HPLC measurements were obtained with a reverse-phase X-bridge C18 column with elution by MeCN-water (40:60) at a flow rate of 1 ml min^{-1} at 25 °C.

S1.2 Materials

Thiazolium catalyst **1** was purchased from Sigma Aldrich and used without further purification. D_2O (99.9 atom % D) and MeOH-d_4 (99.8 atom % D) were purchased from Goss Scientific. $CDCl_3$ (99.8 atom % D) was purchased from Sigma-Aldrich. HPLC grade MeCN and MeOH were purchased from Fisher Scientific. PhCHO and triethylamine (TEA) were purchased from Sigma Aldrich and distilled prior to use. All other reagents were used without further purification. Moisture or air sensitive reactions were carried out under argon in oven-dried glassware. Solvents were dried using an Innovative Technology Inc. solvent purification system.

Triethylamine buffer solutions in MeOH were prepared from distilled TEA and dried triethylamine hydrochloride.

S1.3 Syntheses

Catalysts were synthesised according to our previous publications, based on the procedure of Rovis and co-workers.[S2] All spectroscopic data was consistent with literature data.

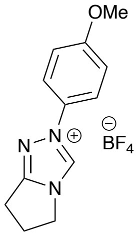

Catalyst **2a**: off-white solid (3.27 g, 72%); m.p. 159–161 °C {lit.3 155–157}; ^{1}H NMR (700 MHz, $CDCl_3$): δ_H 2.87 (2H, m, CH_2), 3.23 (2H, t, J=7.8 Hz, CH_2), 3.86 (3H, s, OCH_3), 4.62 (2H, t, J=7.4 Hz, CH_2), 7.01 (2H, d, J=9.1 Hz, ArH), 7.71 (2H, d, J=9.1 Hz, ArH), 9.97 (1H, s, NCH(N)); ^{13}C NMR (176 MHz, $CDCl_3$): δ_C 22.0 (CH_2), 26.8 (CH_2), 47.8 (CH_2), 55.90 (OCH3), 115.4 (2 × ArCH), 122.8 (2 × ArCH), 128.8 (ArCN), 137.1 (NCH(N)), 161.5 (ArCO), 162.5 (NCN); m/z (ES+): 216 ($[M–BF_4]^+$, 100%); HRMS (ES+): $[M–BF_4]^+$ $C_{12}H_{14}N_3O$ requires 216.1137, found 216.1122.

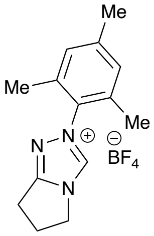

Catalyst **2b:** Procedure altered at arylhydrazine addition by dissolving mesityl hydrazine hydrochloride (1.33 mol eq.) in 1 M NaOH, before extracting into DCM and immediately adding to the reaction, based on work by Smith and co-workers.[S3] Pale brown solid (1.22 g, 66%); m.p. 175–177 °C {lit.4 174–176°C}; ^{1}H NMR (400 MHz, $CDCl_3$): δ_H 2.06 (6H, s, 2 × CH_3), 2.36 (3H, s, CH_3), 2.89 (2H, m, CH_2), 3.25 (2H, t, J=7.7 Hz, CH_2), 4.70 (2H, t, J=7.4 Hz, CH_2), 6.99 (2H, s, 2 × ArCH), 9.51 (1H, s, NCH(N)); ^{13}C NMR (101 MHz, $CDCl_3$): δ_C 17.4 (2 × CH_3), 21.4 (CH_3), 22.1 (CH_2), 26.8 (CH_2), 48.1 (CH_2), 129.8 (2 × ArCH), 132.0 (ArC), 135.3 (2 × ArC), 141.6 (ArC), 142.1 (ArCN), 162.9 (NCN); m/z (ES+): 228 ($[M–BF_4]^+$, 100%).

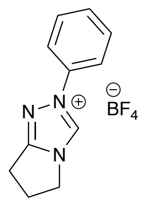

Catalyst **2c**: yellow solid (12.36 g, 81%); m.p. 154–156 °C {lit.3 154–156 °C}; ^{1}H NMR (700 MHz, D_2O): δ_H 2.75 (2H, q, J=7.6 Hz, CH_2), 3.13 (2H, t, J=7.7Hz, CH_2), 4.37 (2H, t, J=7.4 Hz, CH_2), 7.50–7.56 (3H, m, ArH), 7.66 (2H, dd, J=8.1 Hz, ArH), 9.98 (1H, s, NCH(N)); ^{13}C NMR (176 MHz, D_2O): δ_C 21.3 (CH_2), 26.5 (CH_2), 47.3 (CH_2), 121.3 (2 × ArCH), 130.1 (2 × ArCH), 130.9 (ArCH), 135.3 (ArCN), 163.8 (NCN); m/z (ES+): 186 ([M–BF_4]$^+$, 100%).

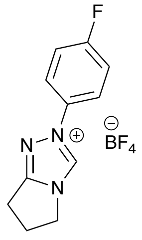

Catalyst **2d**: off-white solid (2.37 g, 58%); m.p. 109–111 °C; ^{1}H NMR (700 MHz, $CDCl_3$): δ_H 2.84 (2H, quintet, J=7.6 Hz, CH_2), 3.21 (2H, t, J=7.4 Hz, CH_2), 4.56 (2H, t, J=7.4 Hz, CH_2), 7.20 (2H, dd, J=9.2, 7.9 Hz, ArH), 7.78 (2H, dd, J=9.2, 4.5 Hz, ArH), 9.92 (1H, s, NCH(N)); ^{13}C NMR (176 MHz, $CDCl_3$): δ_C 21.9 (CH_2), 26.8 (CH_2), 47.7 (CH_2), 117.3 (d, J=23.6 Hz, 2 × ArCH), 123.5 (d, J=9.1, 2 × ArCH), 132.0 (d, J=3.1 Hz, ArCN), 137.8 (NCH(N)), 162.9 (NCN), 164.3 (d, J=251.9 Hz, ArCF); ^{19}F NMR (376 MHz, DMSO-d_6): δ_F –110.7 (ArF), –148.6 (s, BF_4), –148.7 (s, BF_4); ν_{max}/cm^{-1} (neat): 3135, 2357, 1595, 1528, 1514, 1389, 1230, 1030; m/z (ES+): 204 ([M–BF_4]$^+$, 100%); HRMS (ES+): [M–BF_4]$^+$ $C_{11}H_{11}FN_3$ requires 204.0937, found 204.0932.

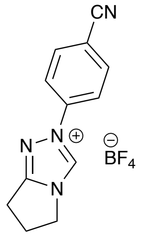

Catalyst **2e**: pale brown solid (1.45 g, 81%); m.p. 125–127 °C; ^{1}H NMR (700 MHz, D_2O): δ_H 2.92 (2H, quintet, J=7.6 Hz, CH_2), 3.31 (2H, t, J=7.6 Hz, CH_2), 4.57 (2H, t, J=7.5 Hz, CH_2), 8.02-8.10 (4H, m, ArH); ^{13}C NMR (125 MHz, D_2O): δ_C 21.6 (CH_2), 26.7 (CH_2), 47.7 (CH_2), 113.5 (ArC), 118.4 (para-CN), 121.8 (2 × ArCH), 134.7 (2 × ArCH), 134.7 (ArCN), 138.8 (NCH(N)), 164.4 (NCN); ν_{max} /cm^{-1} (neat): 3142, 2360, 2244, 1606, 1585, 1523, 1382, 1292, 1222, 1054, 1026; m/z (ES+): 211 ([M–BF_4]$^+$, 100%); HRMS (ES+): [M–BF_4]$^+$ $C_{12}H_{11}N_4$ requires 211.0978, found 211.0979.

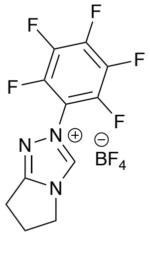

Catalyst **2f**: white solid (1.13 g, 18%); m.p. 250–252 °C {lit.2 248–253 °C}; ^{1}H NMR (500 MHz, MeOD-d_4): δ_H 2.76 (2H, quintet, J=7.4, CH_2),3.16 (2H, t, J=7.8, CH_2), 4.43 (2H, t, J=7.4, CH_2); ^{13}C NMR (125 MHz, MeOD-d_4): δ_C 24.3 (CH_2), 29.2 (CH_2), 58.2 (CH_2), 113.6 (Cq), 139.7 (ArCN), 144.4 (2 × ArCF), 145.3 (ArCF), 146.4 (2 × ArCF), 167.5 (NCN); ^{19}F NMR (400 MHz, $CDCl_3$): δ_F – 146.53 (2F, d, J=19.4, ArF), 147.51 (1F, t, J=21.5, ArF), –150.58 (br s, BF_4), –150.63(q, BF_4), –159.64 (2F, t, J=19.0, ArF); m/z (ES+): 276 ([M–BF_4]$^+$, 100%); HRMS (ES+): [M–BF_4]$^+$ $C_{11}H_7N_3F_5$ requires 276.0566, found 276.0560.

S2 Initial Rate Kinetic Measurements Under Catalytic Conditions

S2.1 Reaction Data and Initial Rate Determination

S 2.1.1.Thiazolium Chloride (**1**)

Table S. 1: Reaction data and initial rates of benzoin formation, catalysed by ***1*** *(30 mM) in 0.16 M TEA-buffered MeOH (66 % f_n) at 50 °C.*

[PhCHO]$_0$	Time / s	[PhCHO] / M	[benzoin] / M	Initial Rate / M s^{-1}
0.32	0	0.32	0	9.39×10^{-7}
	1200	0.318	0.00086	
	2400	0.315	0.00239	
	3300	0.313	0.00328	
	4200	0.312	0.00424	
	5400	0.309	0.00534	
	6300	0.308	0.00604	
	7200	0.306	0.00679	
	8400	0.305	0.00764	
0.64	0	0.64	0	3.07×10^{-6}
	1200	0.634	0.00281	
	2400	0.626	0.00723	
	3300	0.62	0.01008	
	4200	0.614	0.01293	
	5400	0.607	0.01642	
	6300	0.601	0.01942	
	7200	0.596	0.02182	
	8400	0.59	0.02522	
0.96	0	0.96	0	4.92×10^{-6}
	1200	0.951	0.00447	
	2400	0.938	0.01092	
	3300	0.929	0.01532	
	4200	0.92	0.02022	
	5400	0.907	0.0265	
	6300	0.897	0.03153	
	7200	0.891	0.03453	
	8400	0.88	0.03999	
1.28	0	1.28	0	6.29×10^{-6}
	1200	1.268	0.00593	
	2400	1.251	0.01446	
	3300	1.24	0.02022	
	4200	1.227	0.02637	
	5400	1.212	0.03401	
	6300	1.201	0.03932	
	7200	1.188	0.04614	
	8400	1.179	0.05073	
1.6	0	1.6	0	8.80×10^{-6}
	1200	1.583	0.00841	
	2400	1.56	0.01979	
	3300	1.544	0.02801	
	4200	1.527	0.03642	
	5400	1.505	0.04731	
	6300	1.49	0.05484	
	7200	1.475	0.06254	
	8400	1.455	0.07242	

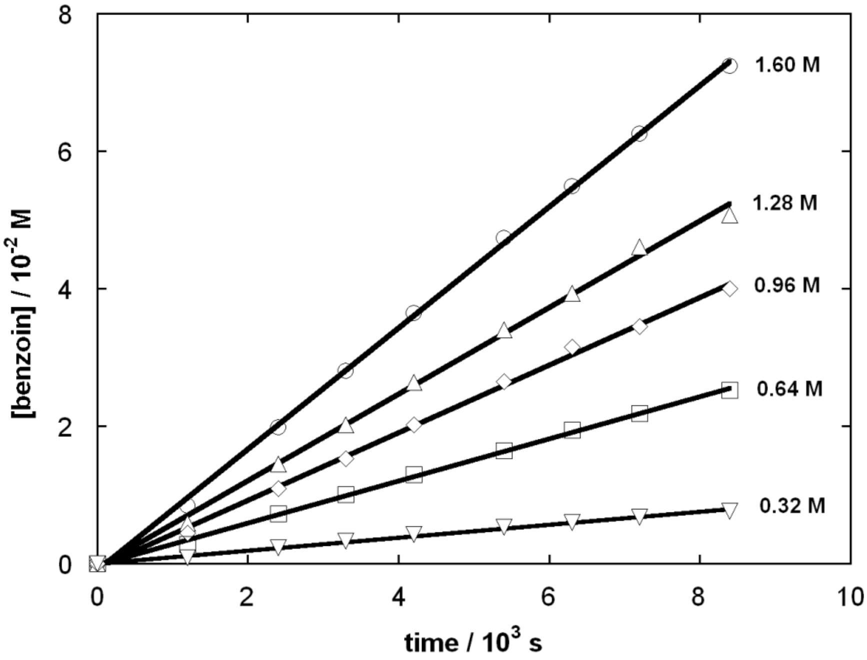

*Figure S. 1: Plots of benzoin concentration vs time for the thiazolium (**1**) (30 mM) catalysed benzoin condensation, at initial benzaldehyde concentrations 0.32 M, 0.64 M, 0.96 M, 1.28 M, 1.60 M*

*Table S. 2: Reaction data and initial rates of benzoin formation, catalysed by **1** (24 mM) in 0.16 M TEA-buffered MeOH (66 % f_n) at 50 °C.*

$[PhCHO]_0$	Time / s	[PhCHO] / M	[benzoin] / M	Initial Rate / M s^{-1}
0.32	0	0.32	0	7.40×10^{-7}
	1200	0.319	0.00061	
	2400	0.317	0.00167	
	3300	0.315	0.00239	
	4200	0.314	0.00313	
	5400	0.312	0.00396	
	6300	0.311	0.00465	
	7200	0.31	0.00524	
	8400	0.308	0.00603	
0.64	0	0.64	0	2.17×10^{-6}
	1200	0.636	0.00185	
	2400	0.63	0.00515	
	3300	0.626	0.00709	
	4200	0.622	0.00897	
	5400	0.616	0.01185	
	6300	0.613	0.01353	
	7200	0.609	0.01541	
	8400	0.604	0.01786	
0.96	0	0.96	0	3.58×10^{-6}
	1200	0.954	0.00307	
	2400	0.944	0.00786	
	3300	0.938	0.01108	
	4200	0.931	0.01428	
	5400	0.923	0.01867	
	6300	0.917	0.02171	
	7200	0.91	0.02499	
	8400	0.901	0.02975	

1.28	0	1.28	0	4.47×10^{-6}
	1200	1.272	0.00412	
	2400	1.259	0.01028	
	3300	1.251	0.01438	
	4200	1.243	0.01859	
	5400	1.232	0.0241	
	6300	1.223	0.02835	
	7200	1.217	0.03166	
	8400	1.207	0.0366	
1.6	0	1.6	0	6.68×10^{-6}
	1200	1.587	0.00627	
	2400	1.57	0.01481	
	3300	1.558	0.02079	
	4200	1.546	0.02697	
	5400	1.529	0.03548	
	6300	1.518	0.04117	
	7200	1.506	0.04716	
	8400	1.489	0.0553	

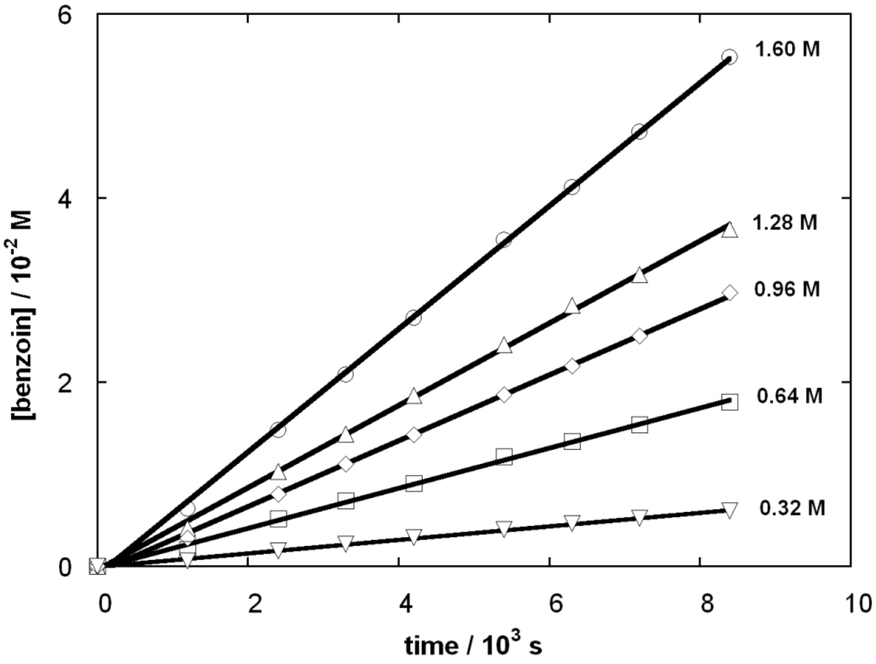

*Figure S. 2: Plots of benzoin concentration vs time for the thiazolium (**1**) (24 mM) catalysed benzoin condensation, at initial benzaldehyde concentrations 0.32 M, 0.64 M, 0.96 M, 1.28 M, 1.60 M*

*Table S. 3: Reaction data and initial rates of benzoin formation, catalysed by **1** (12 mM) in 0.16 M TEA-buffered MeOH (66 % f_n) at 50 °C.*

$[PhCHO]_0$	Time / s	[PhCHO] / M	[benzoin] / M	Initial Rate / M s^{-1}
0.32	0	0.32	0	2.8×10^{-7}
	1200	0.319	0.00029	
	2400	0.319	0.00071	
	3300	0.318	0.00095	
	4200	0.317	0.00127	
	5400	0.317	0.00162	
	6300	0.316	0.00184	
	7200	0.316	0.00211	
	8400	0.315	0.00234	
	9600	0.315	0.00262	
0.64	0	0.64	0	7.06×10^{-7}
	1200	0.638	0.00077	
	2400	0.636	0.00183	
	3300	0.635	0.00253	
	4200	0.634	0.00315	
	5400	0.632	0.00408	
	6300	0.631	0.00453	
	7200	0.629	0.0053	
	8400	0.628	0.00607	
	9600	0.627	0.00661	
0.96	0	0.96	0	1.02×10^{-6}
	1200	0.958	0.00113	
	2400	0.955	0.00261	
	3300	0.953	0.00362	
	4200	0.951	0.00466	
	5400	0.948	0.00589	
	6300	0.947	0.00674	
	7200	0.945	0.00774	
	8400	0.943	0.00871	
	9600	0.941	0.00956	
1.28	0	1.28	0	1.61×10^{-6}
	1200	1.277	0.00151	
	2400	1.273	0.00369	
	3300	1.269	0.00536	
	4200	1.266	0.00686	
	5400	1.263	0.00865	
	6300	1.26	0.01011	
	7200	1.256	0.01176	
	8400	1.253	0.01332	
	9600	1.25	0.01512	
1.6	0	1.6	0	2.61×10^{-6}
	1200	1.595	0.00251	
	2400	1.589	0.00574	
	3300	1.584	0.00818	
	4200	1.579	0.01059	
	5400	1.572	0.01399	
	6300	1.568	0.01613	
	7200	1.563	0.01836	
	8400	1.557	0.0216	

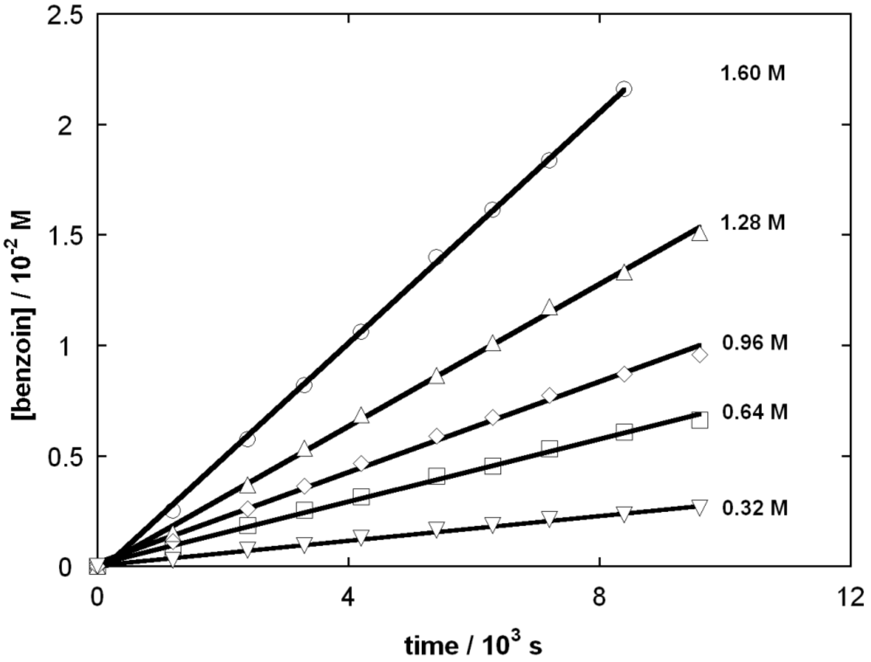

*Figure S. 3: Plots of benzoin concentration vs time for the thiazolium (**1**) (12 mM) catalysed benzoin condensation, at initial benzaldehyde concentrations 0.32 M, 0.64 M, 0.96 M, 1.28 M, 1.60 M*

S 2.1.2.Triazolium Tetrafluoroborate **2a**

*Table S. 4: Reaction data and initial rates of benzoin formation, catalysed by triazolium salt (**2a**) (12 mM) in 0.16 M triethylamine-buffered methanol (66% f_n) at 50 °C.*

$[PhCHO]_0$	Time / s	[PhCHO] / M	[benzoin] / M	Initial Rate / M s^{-1}
0.16	0	0.16	0	1.51×10^{-7}
	2400	0.159	0.00039	
	4800	0.158	0.0008	
	7200	0.158	0.00114	
	9600	0.157	0.00157	
	12000	0.156	0.00185	
	14400	0.156	0.00223	
	16800	0.155	0.00253	
0.32	0	0.32	0	2.79×10^{-7}
	2400	0.319	0.00073	
	4800	0.317	0.00144	
	7200	0.315	0.00229	
	9600	0.314	0.00281	
	12000	0.313	0.00343	
	14400	0.312	0.00401	
	16800	0.31	0.00475	
0.48	0	0.48	0	3.26×10^{-7}
	2400	0.478	0.00083	
	4800	0.477	0.00165	
	7200	0.475	0.00258	
	9600	0.473	0.00341	
	12000	0.472	0.00403	
	14400	0.47	0.00481	
	16800	0.469	0.0054	
0.64	0	0.64	0	3.47×10^{-7}
	2400	0.638	0.00096	
	4800	0.636	0.002	
	7200	0.634	0.00283	
	9600	0.633	0.00372	
	12000	0.631	0.00444	
	14400	0.63	0.00518	
	16800	0.628	0.00582	
0.96	0	0.96	0	3.56×10^{-7}
	2400	0.958	0.00093	
	4800	0.956	0.0021	
	7200	0.954	0.00283	
	9600	0.953	0.00374	
	12000	0.952	0.00409	
	14400	0.949	0.00552	
	16800	0.948	0.006	
1.28	0	1.28	0	3.43×10^{-7}
	2400	1.278	0.00119	
	4800	1.277	0.00171	
	7200	1.275	0.00274	
	9600	1.273	0.00353	
	12000	1.272	0.00423	
	14400	1.27	0.00504	
1.44	0	1.44	0	3.46×10^{-7}
	2400	1.438	0.00096	
	4800	1.436	0.00175	

	7200	1.435	0.00268	
	9600	1.433	0.00367	
	12000	1.432	0.0041	
	14400	1.43	0.00501	
1.6	0	1.6	0	3.53×10^{-7}
	2400	1.598	0.00085	
	4800	1.597	0.00171	
	7200	1.595	0.00269	
	9600	1.593	0.00345	
	12000	1.591	0.00442	

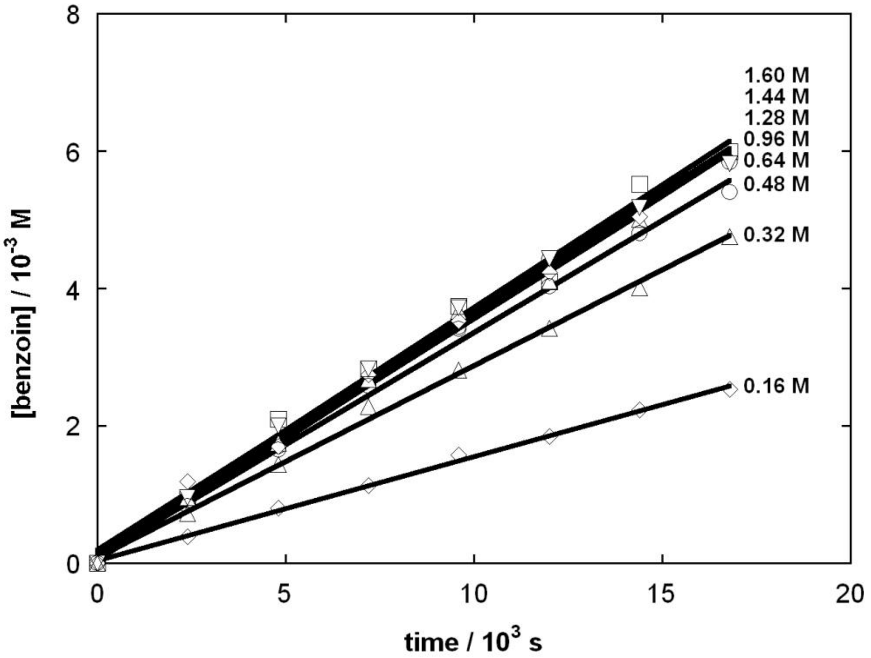

*Figure S. 4: Plots of benzoin concentration against time for the triazolium (**2a**) (12 mM) catalysed benzoin condensation, at initial benzaldehyde concentrations 0.16 M, 0.32 M, 0.48 M, 0.64 M, 0.96 M, 1.28 M, 1.44 M and 1.60 M.*

*Table S. 5: Reaction data and initial rates of benzoin formation, catalysed by triazolium salt (**2a**) (6 mM) in 0.16 M triethylamine-buffered methanol (66% f_n) at 50 °C.*

$[PhCHO]_0$	Time / s	[PhCHO] / M	[benzoin] / M	Initial Rate / M s^{-1}
0.16	0	0.16	0	7.90×10^{-8}
	2400	0.16	0.000213	
	4800	0.159	0.000408	
	7200	0.159	0.00061	
	9600	0.158	0.000807	
	12000	0.158	0.000991	
	14400	0.158	0.001155	
	16800	0.157	0.001324	
0.32	0	0.32	0	1.45×10^{-7}
	2400	0.319	0.000405	
	4800	0.318	0.000803	
	7200	0.318	0.00112	
	9600	0.317	0.001499	
	12000	0.316	0.001842	
	14400	0.316	0.002158	
	16800	0.315	0.002422	
0.48	0	0.48	0	1.78×10^{-7}
	2400	0.479	0.000414	
	4800	0.478	0.000849	
	7200	0.477	0.001283	
	9600	0.477	0.001582	
	12000	0.476	0.002117	
	14400	0.475	0.002609	
0.64	0	0.64	0	1.82×10^{-7}
	2400	0.639	0.000496	
	4800	0.638	0.000895	
	7200	0.637	0.001416	
	9600	0.637	0.001748	
	12000	0.635	0.002273	
	14400	0.635	0.002604	
0.96	0	0.96	0	1.97×10^{-7}
	2400	0.959	0.000519	
	4800	0.958	0.001034	
	7200	0.957	0.001567	
	9600	0.956	0.001999	
	12000	0.955	0.002405	
	14400	0.954	0.002835	
1.28	0	1.28	0	1.89×10^{-7}
	2400	1.279	0.000487	
	4800	1.278	0.001032	
	7200	1.277	0.001489	
	9600	1.276	0.001883	
	12000	1.275	0.002284	
	14400	1.275	0.002744	
1.44	0	1.44	0	1.87×10^{-7}
	2400	1.439	0.000607	
	4800	1.438	0.001085	
	7200	1.437	0.001548	
	9600	1.436	0.001867	
	12000	1.435	0.002379	

	14400	1.435	0.002747	
1.6	0	1.6	0	1.97×10^{-7}
	2400	1.599	0.000608	
	4800	1.598	0.001065	
	9600	1.596	0.001912	
	12000	1.595	0.002479	
	14400	1.594	0.002889	

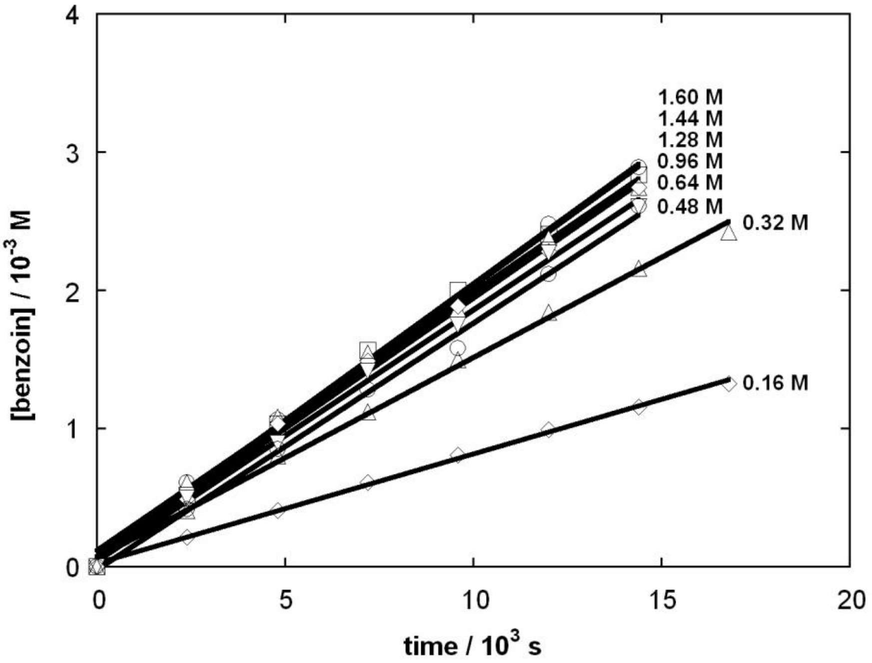

*Figure S. 5: Plots of benzoin concentration against time for the triazolium (**2a**) (6 mM) catalysed benzoin condensation, at initial benzaldehyde concentrations 0.16 M, 0.32 M, 0.48 M, 0.64 M, 0.96 M, 1.28 M, 1.44 M and 1.60 M.*

S 2.1.3. Triazolium Tetrafluoroborate **2b**

*Table S. 6: Reaction data and initial rates of benzoin formation, catalysed by triazolium salt (**2b**) (12 mM) in 0.16 M triethylamine-buffered methanol (66% f_n) at 50 °C.*

$[PhCHO]_0$	Time / s	[PhCHO] / M	[benzoin] / M	Initial Rate / M s^{-1}
0.16	0	0.16	0	2.51×10^{-7}
	1500	0.159	0.00041	
	3000	0.158	0.00077	
	5100	0.157	0.00136	
	6600	0.156	0.00175	
	8700	0.155	0.00226	
	10200	0.155	0.00262	
	11700	0.154	0.00288	
	13200	0.153	0.00335	
0.32	0	0.32	0	4.02×10^{-7}
	1500	0.319	0.00064	
	3000	0.317	0.00132	
	5100	0.316	0.00212	
	6600	0.314	0.00277	
	8700	0.313	0.00353	
	10200	0.312	0.00416	
	11700	0.311	0.00475	
	13200	0.309	0.00535	
0.48	0	0.48	0	4.76×10^{-7}
	1500	0.479	0.00074	
	3000	0.477	0.00151	
	5100	0.475	0.00255	
	6600	0.473	0.00326	
	8700	0.471	0.00437	
	10200	0.47	0.00484	
	11700	0.469	0.00562	
	13200	0.467	0.00628	
0.64	0	0.64	0	5.19×10^{-7}
	1500	0.638	0.00081	
	3000	0.637	0.00163	
	5100	0.634	0.00283	
	6600	0.633	0.00356	
	8700	0.63	0.00475	
	10200	0.629	0.00553	
	11700	0.628	0.00604	
	13200	0.626	0.00679	
0.96	0	0.96	0	5.45×10^{-7}
	1500	0.958	0.00079	
	3000	0.956	0.00183	
	5100	0.954	0.00291	
	6600	0.952	0.00376	
	8700	0.95	0.00476	
	10200	0.949	0.00549	
	11700	0.947	0.00656	
	13200	0.946	0.00722	
1.28	0	1.28	0	5.59×10^{-7}
	1500	1.278	0.00094	
	3000	1.276	0.00178	
	5100	1.274	0.00282	

	6600	1.272	0.00403	
	8700	1.27	0.005	
	10200	1.269	0.00575	
	11700	1.267	0.00668	
	13200	1.265	0.00732	
1.44	0	1.44	0	5.45 × 10^{-7}
	1500	1.438	0.00095	
	3000	1.436	0.00185	
	5100	1.434	0.00304	
	8700	1.43	0.00492	
	10200	1.428	0.00581	
	11700	1.427	0.00639	
	13200	1.425	0.0073	
1.6	0	1.6	0	5.70 × 10^{-7}
	1500	1.599	0.00048	
	3000	1.597	0.00171	
	5100	1.594	0.00283	
	6600	1.592	0.00395	
	8700	1.589	0.00526	
	10200	1.589	0.00567	
	11700	1.587	0.00662	
	13200	1.586	0.00722	

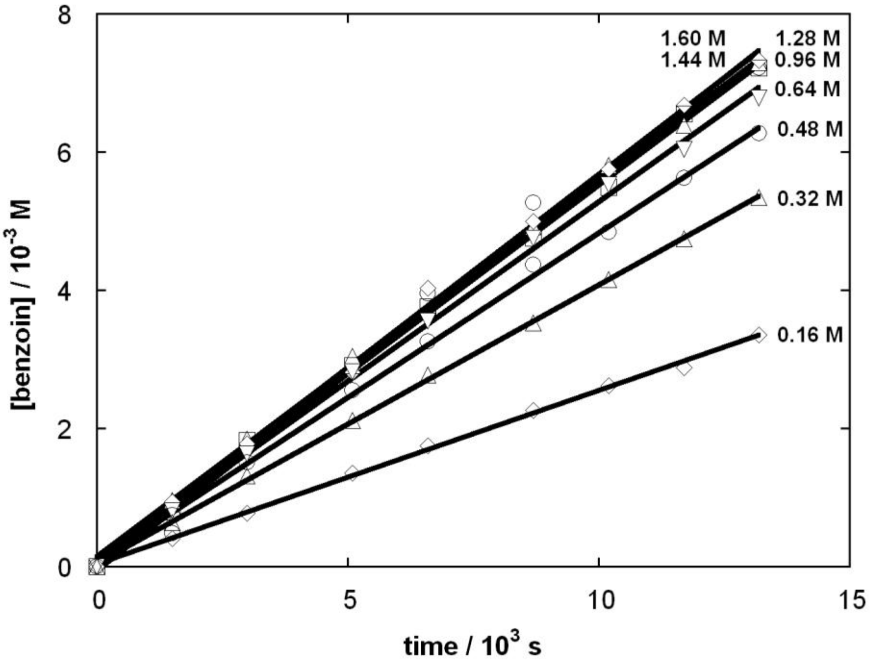

*Figure S. 6: Plots of benzoin concentration against time for the triazolium (**2b**) (12 mM) catalysed benzoin condensation, at initial benzaldehyde concentrations 0.16 M, 0.32 M, 0.48 M, 0.64 M, 0.96 M, 1.28 M, 1.44 M and 1.60 M.*

S 2.1.4.Triazolium Tetrafluoroborate **2c**

*Table S. 7: Reaction data and initial rates of benzoin formation, catalysed by triazolium salt (**2c**) (24 mM) in 0.16 M triethylamine-buffered methanol (66% f_n) at 50 °C.*

$[PhCHO]_0$	Time / s	[PhCHO] / M	[benzoin] / M	Initial Rate / M s^{-1}
0.16	0	0.16	0	3.13×10^{-7}
	1800	0.158	0.0008	
	3600	0.157	0.00134	
	7200	0.155	0.00241	
	9000	0.154	0.00291	
	10800	0.153	0.00351	
	12600	0.152	0.00417	
	14400	0.151	0.00458	
0.32	0	0.32	0	6.76×10^{-7}
	1800	0.317	0.00145	
	3600	0.315	0.00264	
	5400	0.313	0.00373	
	7200	0.31	0.00493	
	9000	0.308	0.0062	
	10800	0.305	0.00748	
	12600	0.304	0.00817	
	14400	0.301	0.00937	
0.64	0	0.64	0	1.03×10^{-6}
	1800	0.636	0.00214	
	3600	0.632	0.00424	
	5400	0.628	0.0061	
	7200	0.624	0.00795	
	9000	0.621	0.00963	
	10800	0.617	0.01151	
	12600	0.613	0.01347	
	14400	0.61	0.01484	
0.96	0	0.96	0	1.20×10^{-6}
	1800	0.955	0.0026	
	3600	0.951	0.00473	
	5400	0.946	0.00682	
	7200	0.942	0.00921	
	9000	0.937	0.01126	
	10800	0.933	0.01357	
	12600	0.929	0.01527	
	14400	0.925	0.01736	
1.28	0	1.28	0	1.30×10^{-6}
	1800	1.274	0.00284	
	3600	1.27	0.00515	
	5400	1.265	0.00744	
	7200	1.26	0.01001	
	9000	1.257	0.01173	
	10800	1.251	0.01462	
	12600	1.247	0.01668	
	14400	1.242	0.01882	
1.44	0	1.44	0	1.34×10^{-6}
	3600	1.429	0.00548	
	5400	1.424	0.00803	
	7200	1.42	0.01025	
	9000	1.415	0.0126	

	10800	1.41	0.01518	
	12600	1.405	0.01727	
	14400	1.401	0.01948	
1.6	0	1.6	0	1.36×10^{-6}
	1800	1.595	0.00256	
	3600	1.59	0.00524	
	5400	1.584	0.00788	
	7200	1.579	0.01028	
	9000	1.574	0.01278	
	12600	1.565	0.01728	
	14400	1.561	0.01962	

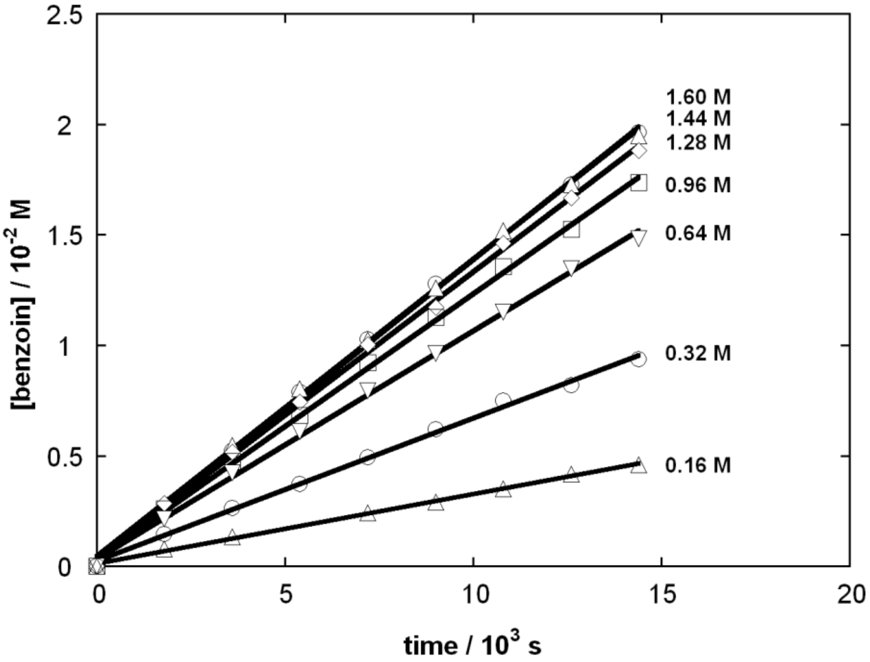

*Figure S. 7: Plots of benzoin concentration against time for the triazolium (**2c**) (24 mM) catalysed benzoin condensation, at initial benzaldehyde concentrations 0.16 M, 0.32 M, 0.64 M, 0.96 M, 1.28 M, 1.44 M, 1.60 M*

*Table S. 8: Reaction data and initial rates of benzoin formation, catalysed by triazolium salt (**2c**) (12 mM) in 0.16 M triethylamine-buffered methanol (66% f_n) at 50 °C.*

[PhCHO]0	Time / s	[PhCHO] / M	[benzoin] / M	Initial Rate, M s^{-1}
0.16	0	0.16	0	2.14×10^{-7}
	1800	0.159	0.00056	
	3600	0.158	0.0009	
	5400	0.157	0.00132	
	9000	0.156	0.00209	
	10800	0.155	0.00239	
	16200	0.153	0.00348	
	19800	0.151	0.00441	
0.32	0	0.32	0	4.33×10^{-7}
	1800	0.318	0.00094	
	5400	0.315	0.00253	
	9000	0.312	0.00399	
	10800	0.31	0.00477	
	16200	0.306	0.00691	
	19800	0.302	0.00879	

0.64	0	0.64	0	6.82×10^{-7}
	1800	0.637	0.00131	
	3600	0.635	0.00269	
	5400	0.632	0.00389	
	9000	0.627	0.00627	
	16200	0.619	0.01071	
	19800	0.612	0.0139	
0.96	0	0.96	0	7.62×10^{-7}
	1800	0.957	0.00166	
	3600	0.954	0.00297	
	5400	0.951	0.00439	
	9000	0.946	0.00711	
	16200	0.936	0.01213	
	19800	0.929	0.01552	
1.28	0	1.28	0	8.04×10^{-7}
	3600	1.274	0.00291	
	5400	1.271	0.00459	
	9000	1.265	0.00739	
	10800	1.262	0.0088	
	16200	1.254	0.01276	
	19800	1.248	0.01618	
1.44	0	1.44	0	8.21×10^{-7}
	1800	1.436	0.00181	
	3600	1.434	0.00319	
	5400	1.431	0.00464	
	9000	1.425	0.00757	
	10800	1.422	0.00898	
	16200	1.415	0.01246	
	19800	1.406	0.01714	
1.6	0	1.6	0	8.07×10^{-7}
	1800	1.596	0.00186	
	3600	1.593	0.00352	
	5400	1.591	0.00466	
	9000	1.586	0.00725	
	10800	1.582	0.00898	
	16200	1.574	0.0131	
	19800	1.567	0.01645	

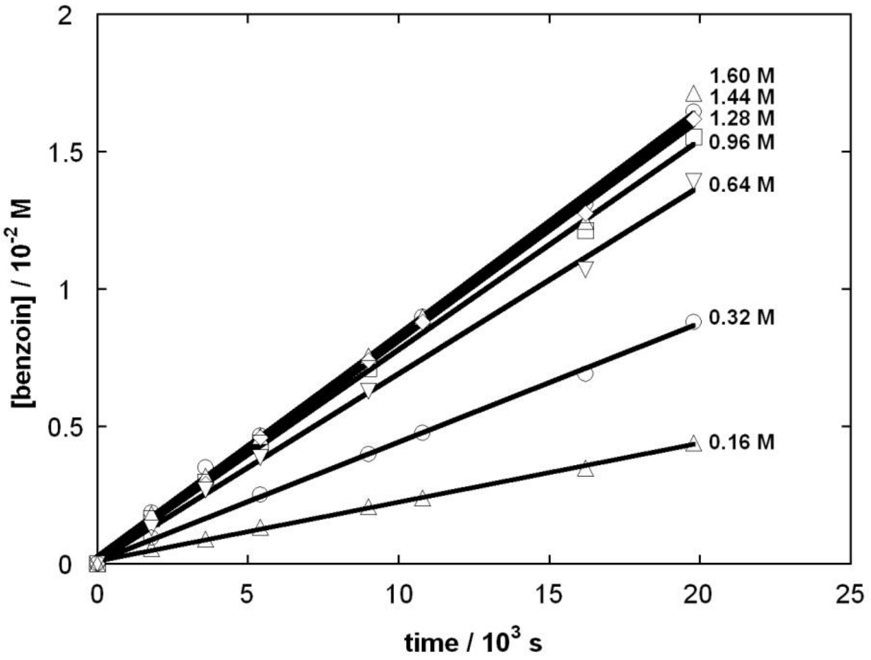

*Figure S. 8: Plots of benzoin concentration against time for the triazolium (**2c**) (12 mM) catalysed benzoin condensation, at initial benzaldehyde concentrations 0.16 M, 0.32 M, 0.64 M, 0.96 M, 1.28 M, 1.44 M, 1.60 M.*

*Table S. 9: Reaction data and initial rates of benzoin formation, catalysed by triazolium salt (**2c**) (6 mM) in 0.16 M triethylamine-buffered methanol(66% f_n) at 50 °C.*

[PhCHO]0	Time / s	[PhCHO] / M	[benzoin] / M	Initial Rate / M s^{-1}
0.16	0	0.16	0	1.18×10^{-7}
	1800	0.159	0.000274	
	3600	0.159	0.000479	
	5400	0.159	0.000688	
	9000	0.158	0.001122	
	10800	0.157	0.001297	
	16200	0.156	0.001875	
	19800	0.155	0.002421	
0.31	0	0.32	0	2.48×10^{-7}
	1800	0.319	0.000596	
	3600	0.318	0.001114	
	5400	0.317	0.001465	
	9000	0.315	0.002333	
	10800	0.314	0.002778	
	16200	0.312	0.004117	
	19800	0.31	0.005023	
0.64	0	0.64	0	3.64×10^{-7}
	1800	0.639	0.000739	
	3600	0.637	0.001465	
	5400	0.636	0.002065	
	9000	0.633	0.003345	
	16200	0.628	0.005859	
	19800	0.625	0.00735	
0.96	0	0.96	0	4.07×10^{-7}
	3600	0.957	0.001532	
	5400	0.955	0.00233	
	9000	0.953	0.003521	
	10800	0.951	0.004511	

	16200	0.947	0.006479	
	19800	0.944	0.00821	
1.28	0	1.28	0	4.13×10^{-7}
	3600	1.277	0.001704	
	5400	1.275	0.002403	
	9000	1.272	0.003957	
	10800	1.271	0.004622	
	16200	1.267	0.00653	
	19800	1.263	0.008437	
1.44	0	1.44	0	4.18×10^{-7}
	3600	1.436	0.001824	
	5400	1.435	0.002572	
	9000	1.432	0.003925	
	10800	1.431	0.004679	
	16200	1.426	0.006795	
	19800	1.423	0.008537	
1.6	0	1.6	0	4.25×10^{-7}
	3600	1.596	0.001962	
	5400	1.694	0.002851	
	9000	1.592	0.004064	
	10800	1.59	0.004799	
	16200	1.586	0.006906	
	19800	1.582	0.008816	

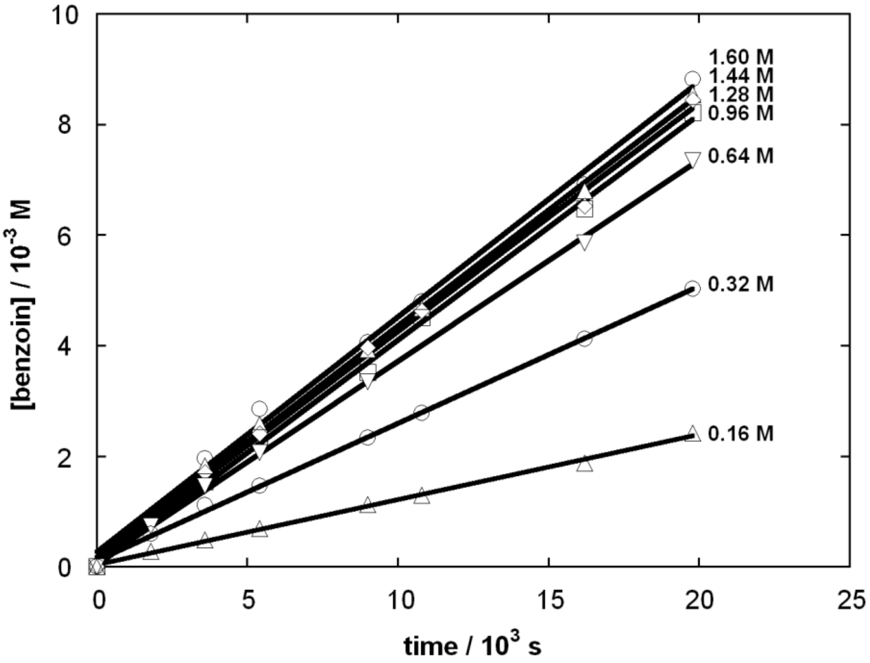

*Figure S. 9: Plots of benzoin concentration against time for the triazolium (**2c**) (6 mM) catalysed benzoin condensation, at initial benzaldehyde concentrations 0.16 M, 0.32 M, 0.64 M, 0.96 M, 1.28 M, 1.44 M, 1.60 M*

S 2.1.5. Triazolium Tetrafluoroborate **2d**

*Table S. 10: Reaction data and initial rates of benzoin formation, catalysed by triazolium salt (**2d**) (12 mM) in 0.16 M triethylamine-buffered methanol (66% f_n) at 50 °C.*

$[PhCHO]_0$	Time / s	[PhCHO] / M	[benzoin] / M	Initial Rate / M s^{-1}
0.16	0	0.16	0.16	5.52×10^{-7}
	1800	0.158	0.158	
	3600	0.156	0.156	
	5400	0.154	0.154	
	7200	0.152	0.152	
	9000	0.15	0.15	
0.32	0	0.32	0	9.72×10^{-7}
	1800	0.316	0.00188	
	3600	0.313	0.00363	
	5400	0.309	0.00545	
	7200	0.306	0.00711	
	9000	0.303	0.00874	
0.64	0	0.64	0	1.27×10^{-6}
	1800	0.635	0.00255	
	3600	0.63	0.00493	
	5400	0.626	0.00712	
	7200	0.621	0.0093	
	9000	0.617	0.0115	
0.96	0	0.96	0	1.36×10^{-6}
	1800	0.954	0.00283	
	3600	0.95	0.00521	
	5400	0.945	0.00757	
	7200	0.94	0.0101	
	9000	0.935	0.01228	
1.28	0	1.28	0	1.36×10^{-6}
	1800	1.275	0.00272	
	3600	1.27	0.00517	
	5400	1.265	0.00765	
	7200	1.26	0.00986	
	9000	1.255	0.01229	
1.44	0	1.44	0	1.35×10^{-6}
	1800	1.435	0.00262	
	3600	1.43	0.0052	
	5400	1.425	0.00741	
	7200	1.42	0.00977	
1.6	0	1.6	0	1.35×10^{-6}
	1800	1.594	0.00288	
	3600	1.59	0.00517	
	5400	1.585	0.00742	
	7200	1.58	0.00985	

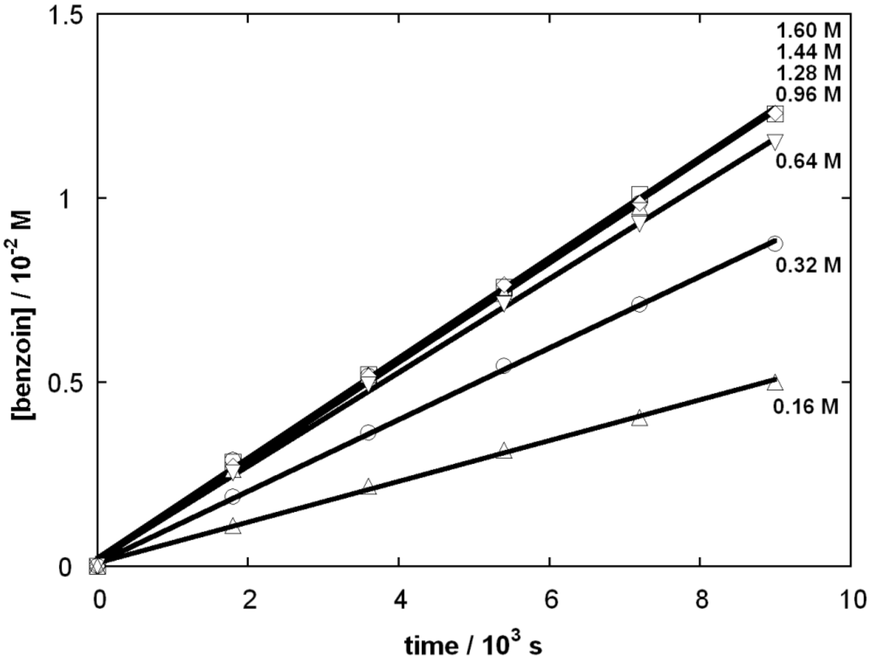

*Figure S. 10: Plots of benzoin concentration against time for the triazolium (**2d**) (12 mM) catalysed benzoin condensation, at initial benzaldehyde concentrations 0.16 M, 0.32 M, 0.64 M, 0.96 M, 1.28 M, 1.44 M, 1.60 M.*

S 2.1.6. Triazolium Tetrafluoroborate **2e**

*Table S. 11: Reaction data and initial rates of benzoin formation, catalysed by triazolium salt (**2e**) (12 mM) in 0.16 M triethylamine-buffered methanol (66% f_n) at 50 °C.*

$[PhCHO]_0$	Time / s	[PhCHO] / M	[benzoin] / M	Initial Rate / M s^{-1}
0.16	0	0.16	0	1.51×10^{-6}
	600	0.158	0.001	
	1320	0.156	0.00216	
	1800	0.154	0.00303	
	2400	0.152	0.00392	
	2700	0.151	0.00434	
	3000	0.151	0.00473	
	3600	0.149	0.00549	
	4200	0.147	0.00632	
0.32	0	0.32	0	3.19×10^{-6}
	480	0.317	0.00167	
	1200	0.312	0.00414	
	1680	0.308	0.00588	
	2280	0.305	0.00769	
	2580	0.303	0.00864	
	2880	0.301	0.0096	
	3480	0.297	0.01129	
	4080	0.294	0.01291	
0.48	0	0.48	0	4.53×10^{-6}
	360	0.477	0.00169	
	1080	0.468	0.00575	
	2160	0.459	0.0105	
	2460	0.457	0.01172	
	2760	0.454	0.01286	
	3360	0.449	0.01554	
	3960	0.444	0.01786	
0.8	0	0.8	0	6.36×10^{-6}
	300	0.796	0.00196	
	780	0.789	0.0056	
	1200	0.783	0.00856	
	1500	0.78	0.01018	
	1920	0.774	0.01278	
	2400	0.769	0.01564	
	2700	0.765	0.01733	
	3000	0.762	0.01917	
1.12	0	1.12	0	7.49×10^{-6}
	300	1.115	0.00229	
	780	1.108	0.00603	
	1200	1.101	0.0096	
	1500	1.096	0.01194	
	1920	1.091	0.01453	
	2400	1.084	0.01814	
	2700	1.08	0.02021	
	3000	1.075	0.02265	
1.28	0	1.28	0	7.93×10^{-6}
	600	1.27	0.00486	
	900	1.265	0.00745	
	1200	1.261	0.00953	
	1500	1.255	0.01226	

	1800	1.251	0.01446	
	2100	1.247	0.01632	
	2400	1.241	0.01933	
1.44	0	1.44	0	8.19×10^{-6}
	300	1.434	0.00312	
	600	1.43	0.00511	
	900	1.425	0.00755	
	1200	1.419	0.01043	
	1500	1.415	0.01257	
	1800	1.411	0.01464	
	2100	1.404	0.01785	
	2400	1.4	0.0198	
1.6	0	1.6	0	8.36×10^{-6}
	300	1.595	0.00258	
	600	1.59	0.00525	
	900	1.584	0.0078	
	1200	1.579	0.01049	
	1500	1.574	0.01321	
	1800	1.569	0.01548	
	2100	1.565	0.01769	
	2400	1.56	0.0198	

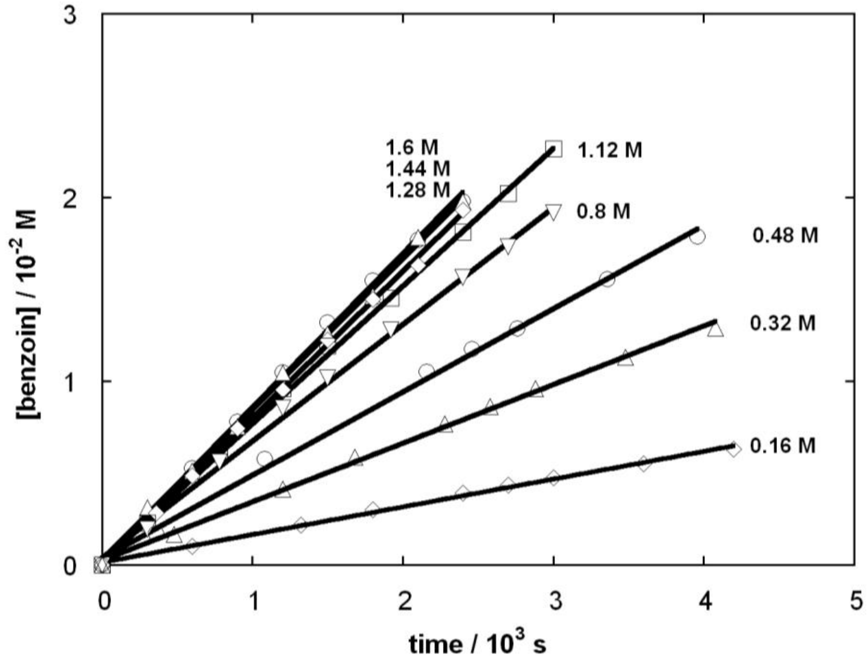

*Figure S. 11: Plots of benzoin concentration against time for the triazolium (**2e**) (12 mM) catalysed benzoin condensation, at initial benzaldehyde concentrations 0.16 M, 0.32 M, 0.48 M, 0.80 M, 1.12 M, 1.28 M, 1.44 M and 1.60 M.*

S 2.1.7.Triazolium Tetrafluoroborate **2f**

*Table S. 12: Reaction data and initial rates of benzoin formation, catalysed by triazolium salt (**2f**) (6 mM) in 0.16 M triethylamine-buffered methanol (66% f_n) at 50 °C.*

$[PhCHO]_0$	Time / s	[PhCHO] / M	[benzoin] / M	Initial Rate / M s^{-1}
0.16	0	0.16	0	7.14×10^{-6}
	90	0.158	0.00078	
	180	0.157	0.00142	
	270	0.156	0.0021	
	360	0.154	0.00278	
	450	0.153	0.00341	
	540	0.152	0.00408	
	630	0.151	0.00464	
	720	0.15	0.00508	
0.32	0	0.32	0.00000931	9.31×10^{-6}
	90	0.318	0.00076	
	180	0.317	0.00165	
	270	0.315	0.00258	
	360	0.313	0.00353	
	450	0.312	0.00422	
	540	0.31	0.00516	
	630	0.308	0.00584	
	720	0.307	0.00659	
0.48	0	0.48	0	1.11×10^{-5}
	60	0.479	0.0006	
	120	0.477	0.0014	
	180	0.476	0.00221	
	270	0.474	0.00317	
	360	0.472	0.00415	
	450	0.47	0.00513	
	540	0.468	0.00622	
	630	0.466	0.00724	
	720	0.464	0.00779	
0.64	0	0.64	0	1.21×10^{-5}
	60	0.639	0.00072	
	120	0.637	0.00164	
	180	0.635	0.00253	
	270	0.633	0.00353	
	360	0.631	0.00464	
	450	0.629	0.00572	
	540	0.626	0.00677	
	630	0.625	0.0077	
	720	0.623	0.00871	
0.96	0	0.96	0	1.40×10^{-5}
	60	0.958	0.00116	
	120	0.956	0.00188	
	180	0.955	0.00263	
	240	0.953	0.00343	
	300	0.951	0.00442	
	360	0.95	0.00503	
	420	0.948	0.00619	
	480	0.946	0.00683	
	540	0.945	0.00769	
1.28	0	1.28	0	

	60	1.279	0.00075	1.40×10^{-5}
	120	1.277	0.0016	
	180	1.275	0.00233	
	240	1.273	0.00341	
	300	1.272	0.00409	
	360	1.27	0.00489	
	420	1.268	0.00591	
	480	1.267	0.00632	
	540	1.265	0.00754	
	600	1.263	0.00844	
1.44	0	1.44	0	1.45×10^{-5}
	60	1.438	0.00107	
	120	1.436	0.00194	
	180	1.434	0.00276	
	240	1.433	0.0035	
	300	1.431	0.00443	
	360	1.429	0.00535	
	420	1.428	0.00614	
	480	1.426	0.00714	
	540	1.424	0.00788	
	600	1.422	0.00881	
1.6	0	1.6	0	1.51×10^{-5}
	60	1.598	0.00107	
	120	1.597	0.0017	
	180	1.594	0.00289	
	240	1.593	0.00361	
	300	1.59	0.00477	
	420	1.587	0.00628	
	480	1.585	0.00732	
	540	1.583	0.00831	
	600	1.582	0.00913	

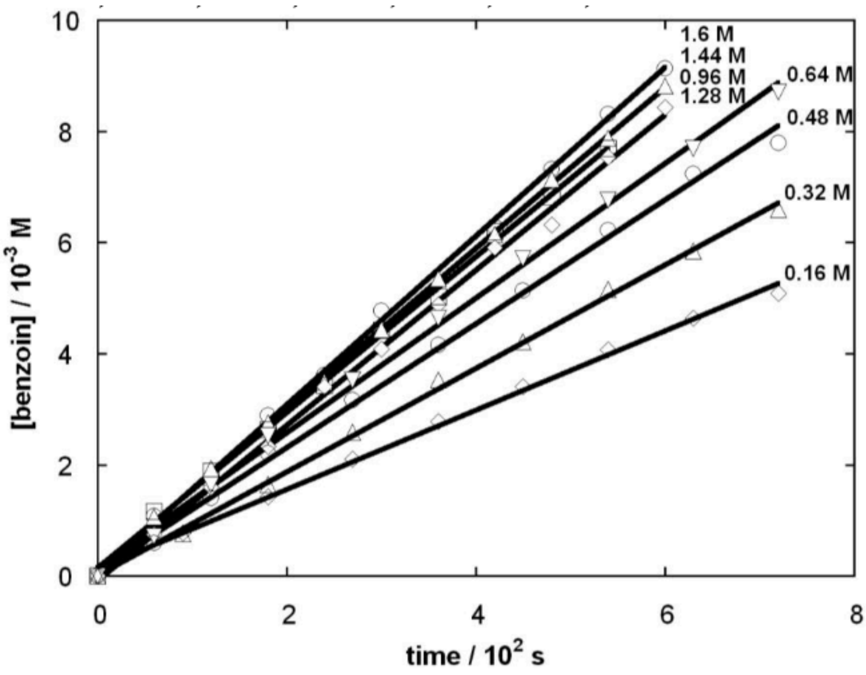

*Figure S. 12: Plots of benzoin concentration against time for the triazolium (**2f**) (6 mM) catalysed benzoin condensation, at initial benzaldehyde concentrations 0.16 M, 0.32 M, 0.48 M, 0.64 M, 0.96 M, 1.28 M, 1.44 M and 1.60 M.*

S2.2 Initial Rate Plots versus $[PhCHO]_0$ and Steady State Kinetic Fitting

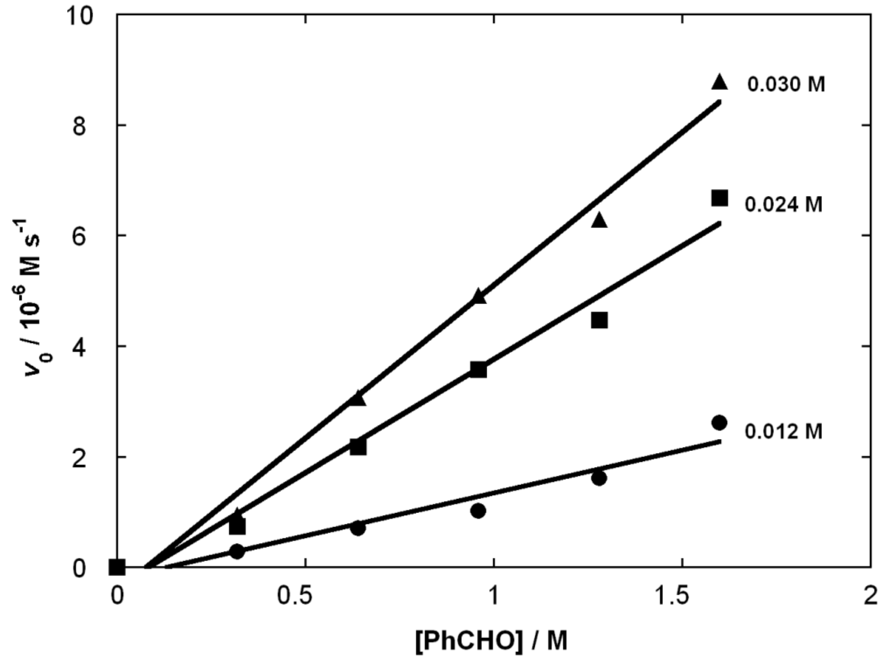

*Figure S. 13: Initial rate vs $[PhCHO]_0$ for thiazolium chloride **1** at 12, 24 and 30 mM pre-catalyst concentrations, determined from monitoring benzoin formation over time at < 10 % conversion. Solid lines show kinetic fits to equation (1).*

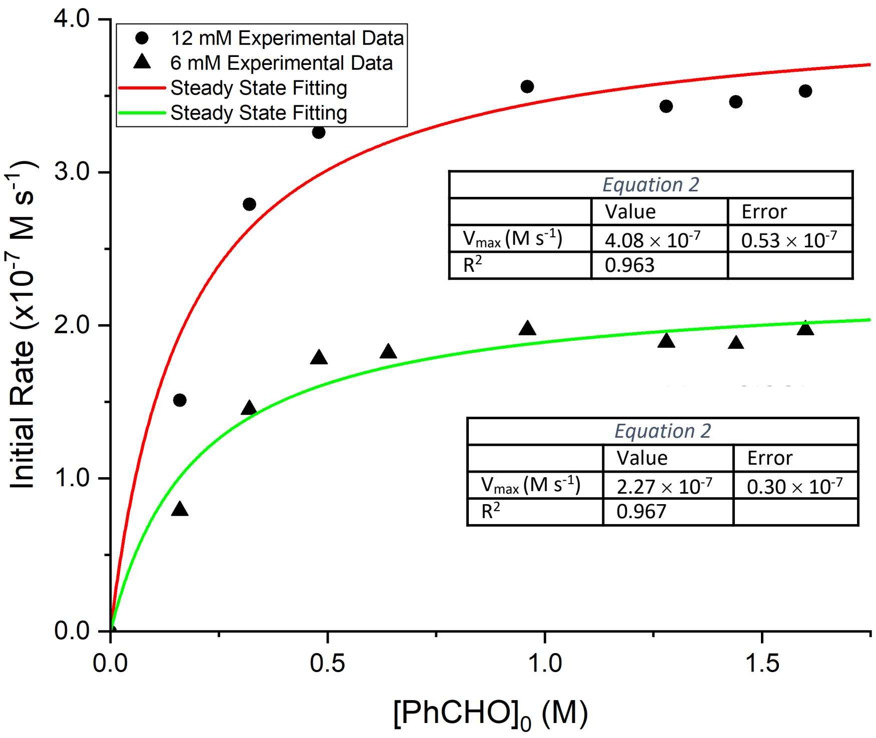

Equation 2		
	Value	Error
V_{max} (M s^{-1})	4.08×10^{-7}	0.53×10^{-7}
R^2	0.963	

Equation 2		
	Value	Error
V_{max} (M s^{-1})	2.27×10^{-7}	0.30×10^{-7}
R^2	0.967	

*Figure S. 14: Initial rate vs $[PhCHO]_0$ for triazolium tetrafluoroborate **2a** at 12 and 6 mM pre-catalyst concentrations, determined from monitoring benzoin formation over time at < 10 % conversion. Coloured lines show kinetic fits to equation (2) .*

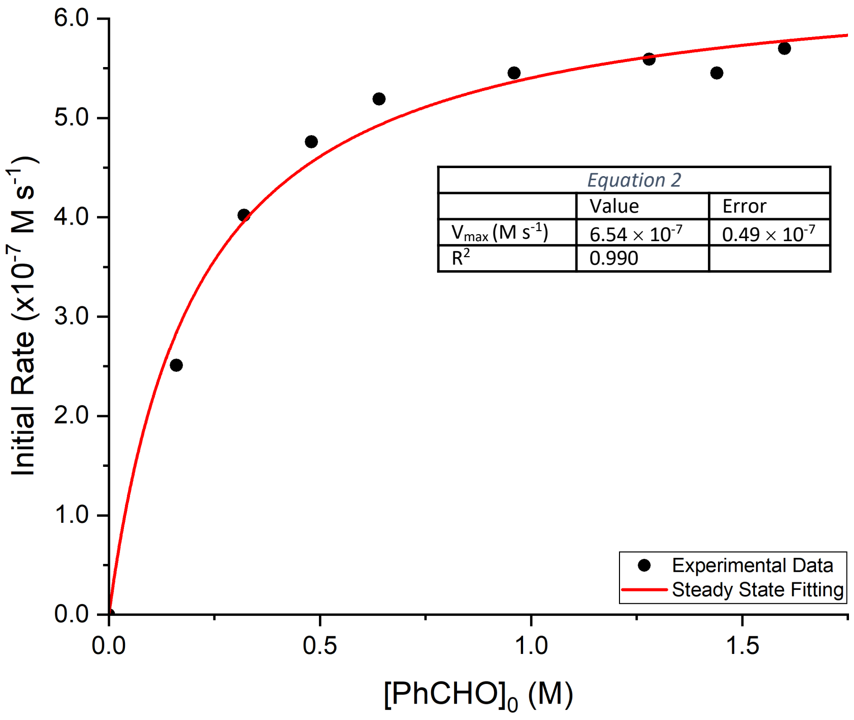

*Figure S. 15: Initial rate vs [PhCHO]$_0$ for triazolium tetrafluoroborate **2b** at 12 mM pre-catalyst concentration, determined from monitoring benzoin formation over time at <10 % conversion. The red line shows the kinetic fit to equation (2).*

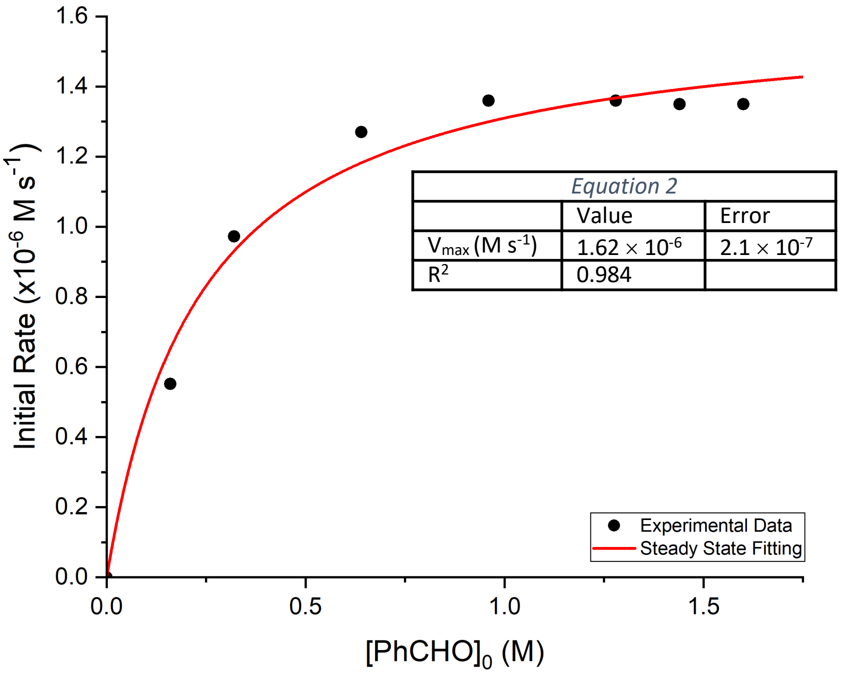

*Figure S. 16: Initial rate vs [PhCHO]$_0$ for triazolium tetrafluoroborate **2d** at 12 mM pre-catalyst concentrations, determined from monitoring benzoin formation over time at <10 % conversion. The red line shows the kinetic fit to equation (2).*

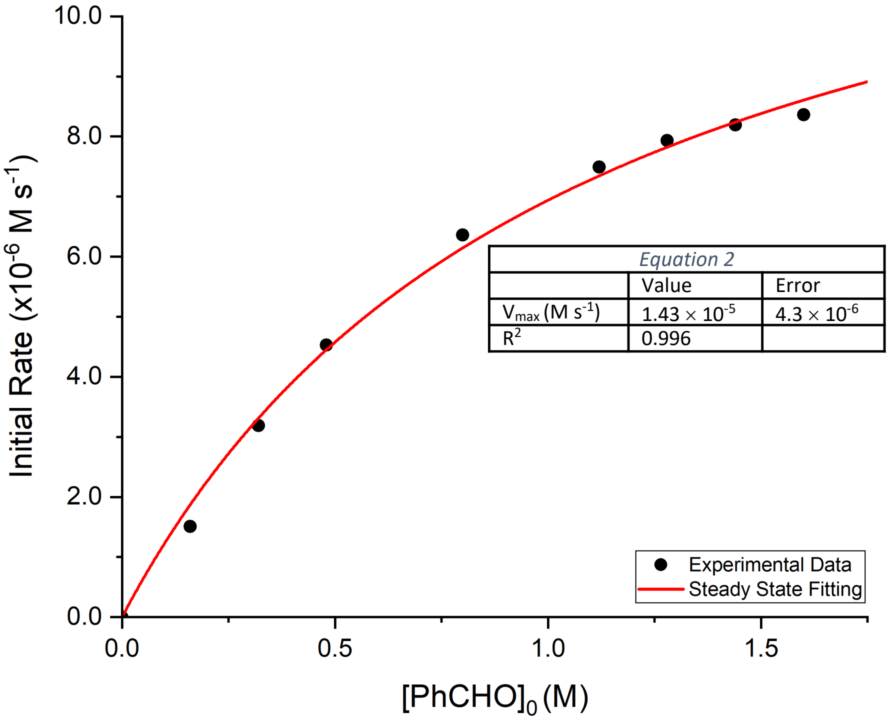

Equation 2		
	Value	Error
V_{max} (M s^{-1})	1.43 × 10^{-5}	4.3 × 10^{-6}
R^2	0.996	

*Figure S. 17: Initial rate vs [PhCHO]$_0$ for triazolium tetrafluoroborate **2e** at 12 mM pre-catalyst concentrations, determined from monitoring benzoin formation over time at <10 % conversion. The red line shows the kinetic fit to equation (2).*

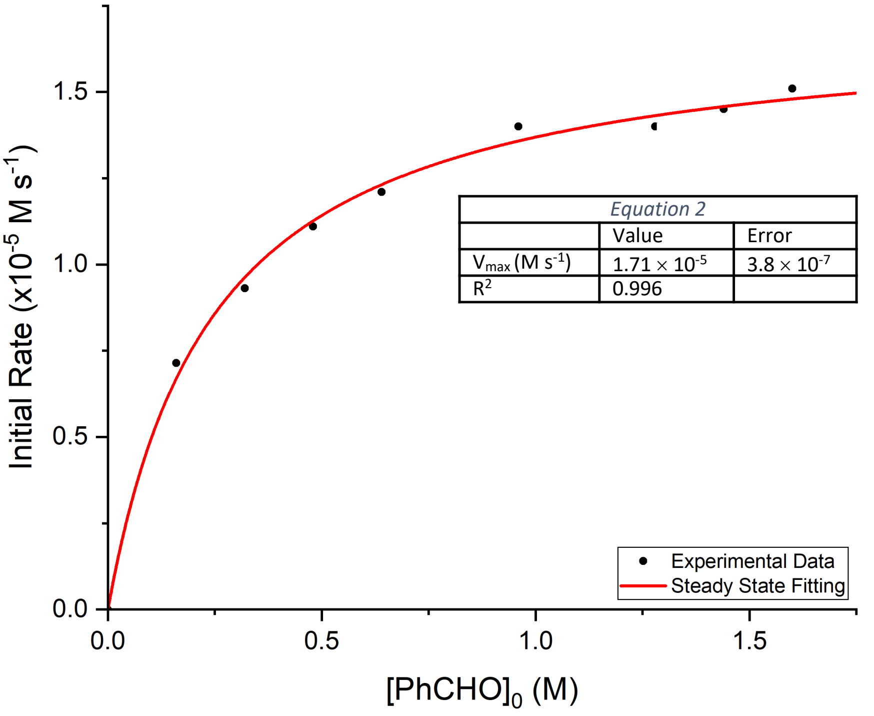

Equation 2		
	Value	Error
V_{max} (M s^{-1})	1.71 × 10^{-5}	3.8 × 10^{-7}
R^2	0.996	

*Figure S. 18: Initial rate vs [PhCHO]$_0$ for triazolium tetrafluoroborate **2f** at 6 mM pre-catalyst concentrations, determined from monitoring benzoin formation over time at <10 % conversion. The red line shows the kinetic fit to equation (2).*

S3 Determination of k_{BI} from Concentration Profiles under Stoichiometric Conditions.

Previously we have reported the determination of rate and equilibrium constants for adduct **III** formation from benzaldehyde and triazolium catalysts **2a-d** by ^{1}H NMR analysis under stoichiometric conditions at 25 °C in triethylamine-buffered d$_3$-methanol.[S4] NMR analysis of the concentration of species over time permitted the calculation of concentration profiles which could be quantitatively fitted to determine rate and equilibrium constants. From these concentration profiles, you can also observe the slow decay of adduct **III** over time to benzoin product and α-deuterated adduct d-**III**. As Breslow intermediate **IV** is not observed by ^{1}H NMR under these reaction conditions, it can be assumed that decay of adduct towards products is limited by BI formation. In our previous publication[S4] we further analysed the concentration profiles to access k_2 (attributable to k_{BI}) just in the case of triazolium catalyst **2c**. Herein we also report k_2 for **2a**, **2b** and **2d** using the data/concentration profiles in our previous publication.[S4] The expression for the rate of forward adduct consumption is given in Equation S.1 and the integrated rate equation is shown in Equation S. 2.

$$-\frac{d[\boldsymbol{III}(H)]}{dt} = k_{BI}^{stoich}[\boldsymbol{III}(H)] \qquad \textit{Equation S. 1}$$

$$[\boldsymbol{III}(H)] = [\boldsymbol{III}(H)]_0 e^{-k_{BI}^{stoich}t} \qquad \textit{Equation S. 2}$$

A value of k_{BI}^{stoich} may be obtained from the slope of a semilogarithmic plot of the concentration of the respective protonated form of the adduct **(III)** against time (Figures S. 19-S. 21). Values for k_{BI}^{stoich} are summarised in Table S. 13. As only the early stage of adduct decay towards products was monitored (well short of the normal 3-5 $t_{1/2}$ of reaction desirable for accurate fitting of a first order process), these k_{BI}^{stoich} values are estimates.

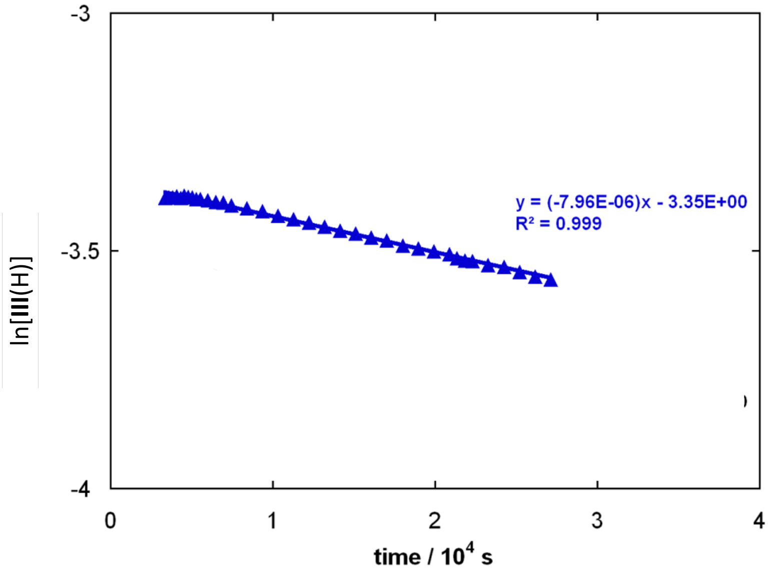

*Figure S. 19: Semilogarithmic plots of [**III**(H)] against time for the reaction of benzaldehyde with triazolium precatalyst (**2a**)*

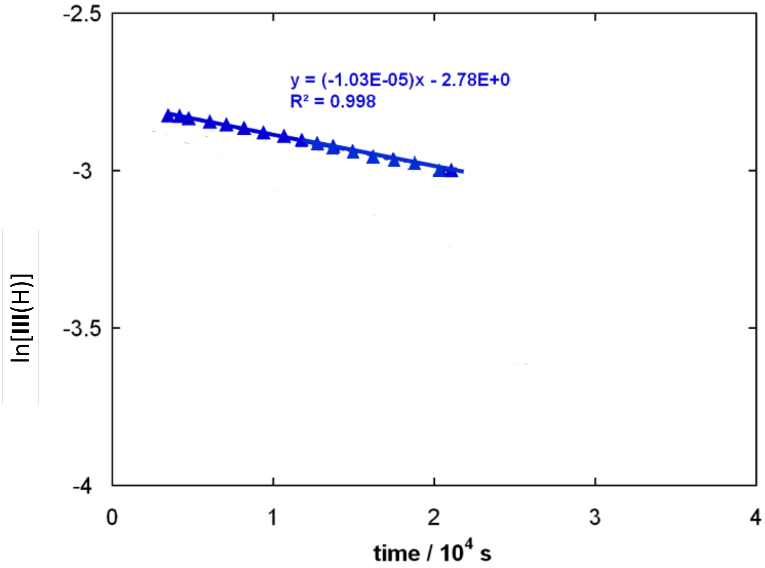

*Figure S. 20: Semilogarithmic plots of [**III**(H)] against time for the reaction of benzaldehyde with triazolium precatalyst (**2b**)*

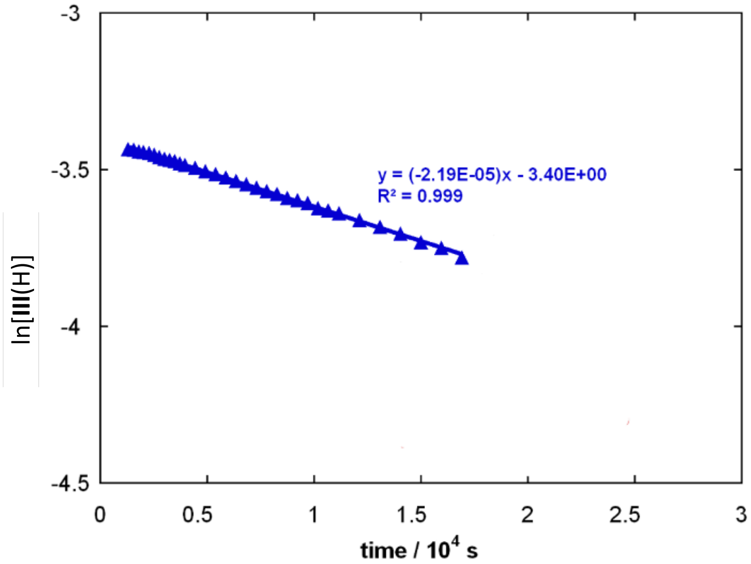

*Figure S. 21: Semilogarithmic plots of [**III**(H)] against time for the reaction of benzaldehyde with triazolium precatalyst (**2d**).*

Table S. 13: Summary of values obtained for k_2 at 25 °C from the manual fitting shown in Figures S. 43-S. 46.

Catalyst	k_{BI}^{stoich} / s^{-1}	k_{BI}^{stoich}(rel.)
2a	7.96 × 10^{-6}	0.84
2b	1.03 × 10^{-5}	1.1
2c[a]	9.45 × 10^{-6}	1.0
2d	2.19 × 10^{-5}	2.3

[a] Value previously published.[S4]

Values for k_{BI}^{stoich} determined above from the stoichiometric experiments at 25 °C are ~10-fold smaller than values reported herein in the main manuscript for $\nu_{max}/[\mathbf{I}] = k_{BI}$ at 50 °C for the same catalysts **2a-d**, which is consistent with the ~10-fold change in rate constant expected for a 25 °C change in temperature and an Arrhenius temperature dependence. The k_{BI}^{stoich} (rel) values are in remarkable agreement with the k_{BI}^{rel} values in the main manuscript, which is further good evidence that BI-formation (conversion of **III** to **IV**) is the rate-limiting step attributable to the plateau region of the initial rate plots.

S4 Steady State Equation Derivation and Validity

S4.1 Derivation of the Steady State Equation

With reference to Scheme 1 in the main manuscript:

$$\text{rate}=k_p[\mathbf{IV}][\text{PhCHO}]$$

$$\frac{d[\mathbf{IV}]}{dt}=k_{BI}[\mathbf{III}] - k_{-BI}[\mathbf{IV}] - k_p[\mathbf{IV}][\text{PhCHO}]$$

At steady state it is assumed:

$$\frac{d[\mathbf{IV}]}{dt} = 0$$

$$=> k_{BI}[\mathbf{III}] - k_{-BI}[\mathbf{IV}] - k_p[\mathbf{IV}][\text{PhCHO}] = 0$$

$$\therefore [\mathbf{IV}]= \frac{k_{BI}[\mathbf{III}]}{k_{-BI}+ k_p[\text{PhCHO}]}$$

Under conditions of high [PhCHO] and low catalyst, assume that: [**III**] = [**I**]

$$=> [\mathbf{IV}] = \frac{k_{BI}[\mathbf{I}]}{k_{-BI} + k_p[\text{PhCHO}]}$$

$$\therefore \text{rate} = \frac{k_{BI}k_p[\mathbf{I}][\text{PhCHO}]}{k_{-BI} + k_p[\text{PhCHO}]} = \frac{k_p v_{max}[\text{PhCHO}]}{k_{-BI} + k_p[\text{PhCHO}]}$$

S4.2 Validity of the Steady State Fit and Assumption [**III**]=[**I**]

S 4.2.1. Half-life Determination for Equilibration of Triazolium Catalysts **2a-d**, Benzaldehyde and Adduct **III** in the Forward Direction

Half-lives were determined using Equation S. 3, derived considering the reversibility of adduct formation[S4, S5], by first calculating x_1 and x_2, the routes of quadratic determined from integration of the differential rate equation for approaching equilibrium for adduct formation in the forward direction. These values are obtained by inputting the equilibrium constant (K_1) values and intial catalyst and benzaldehyde concentrations for a certain catalyst/aldehyde system. These values are then used in the key equation to determine the $t_{1/2}$ by setting $x = [\mathrm{cat}]_0/2$ (as the limiting reagent) before dividing through by k_1 to obtain a value to $t_{1/2}$. Half-lives determined are summarised in Table S. 14.

*Equation S. 3: Formula used to determine the half-lives of initial adduct formation from catalyst for **2a-d** at 25 ℃ using values of K_1 and k_1 from studies at stoichiometric catalyst concentrations[4,5]: $x_0 = [\mathrm{cat}]_0$, $y_0 = [\mathrm{PhCHO}]_0$, $x = [\mathrm{cat}]$, t = time, k_1 = rate constant for adduct formation, K = equilibrium constant for adduct formation.*

$$k_1 t = \frac{1}{\sqrt{\left(y_0 - x_0 + \frac{1}{K}\right)^2 + \frac{4x_0}{K}}} \left| \ln\left(\frac{x - x_1}{x - x_2}\right) \right| \Bigg|_{x_0}^{x}$$

$$x_1 = \frac{-\left(y_0 - x_0 + \frac{1}{K}\right) + \sqrt{\left(y_0 - x_0 + \frac{1}{K}\right)^2 + \frac{4x_0}{K}}}{2}$$

$$x_2 = \frac{-\left(y_0 - x_0 + \frac{1}{K}\right) - \sqrt{\left(y_0 - x_0 + \frac{1}{K}\right)^2 + \frac{4x_0}{K}}}{2}$$

S 4.2.2. Berkeley-Madonna Global Fitting – Determination of % Free Catalyst at Equilibrium

Using rate constants determined at stoichiometric concentrations of triazolium catalysts **2a-d** and benzaldehyde, as described in our previous work[S4], the percentage free catalyst was determined through use of Berkeley-Madonna Software. A representative selection of plots is shown below (Figure S. 22).

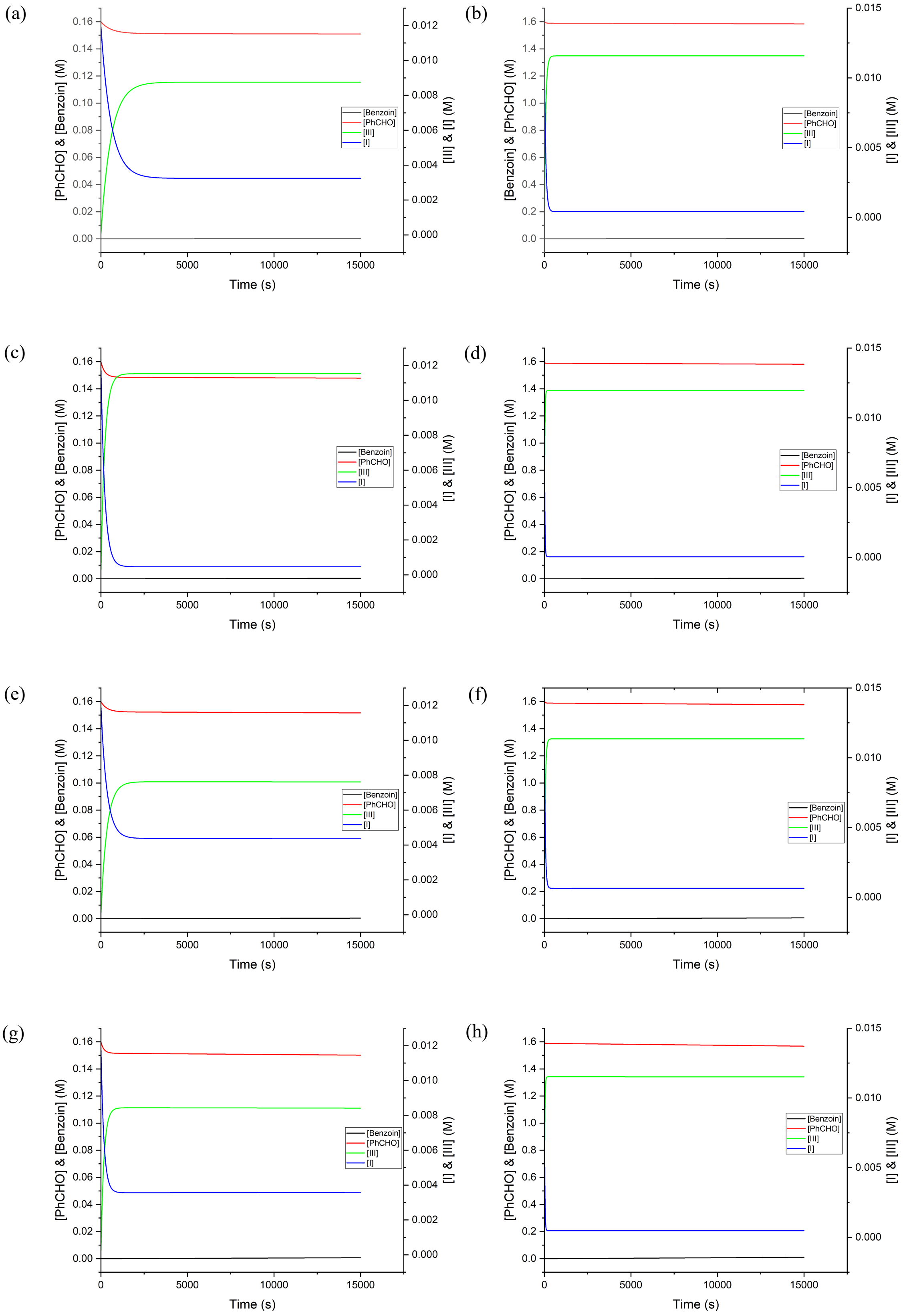

*Figure S. 22: Plots of concentration of benzaldehyde (red), benzoin (black), catalyst (blue) and adduct (green) over time, plotted using Berkeley-Madonna software with values for rate constants determined at stoichiometric catalyst concentration as described in Section **S3**, for catalyst concentrations of 12 mM. (a) Catalyst **2a**, [PhCHO]$_0$ = 0.16 M, (b) Catalyst **2a**, [PhCHO]$_0$ = 1.6 M; (c) Catalyst **2b**, [PhCHO]$_0$ = 0.16 M, (d) Catalyst **2b**, [PhCHO]$_0$ = 1.6 M; (e) Catalyst **2c**, [PhCHO]$_0$ = 0.16 M, (f) Catalyst **2c**, [PhCHO]$_0$ = 1.6 M; (g) Catalyst **2d**, [PhCHO]$_0$ = 0.16 M, (h) Catalyst **2d**, [PhCHO]$_0$ = 1.6 M.*

S 4.2.3.Summary Table

Table S. 14: Summary of half-lives and % free catalyst at equilibrium determined through use of rate constants and equilibrium constants determined under stoichiometric conditions at 25 ºC.

Catalyst	Catalyst Concentration / M	Benzaldehyde Concentration / M	$k_1^{a,b}$ / M s^{-1}	$k_{-1}^{a,c}$ / s^{-1}	k_{BI}^{d} / s^{-1}	$K_1^{a,e}$ / M	% Free Catalyst at Equilibrium[f]	Half Life[g] / s
2a	0.012	0.16	7.92×10^{-3}	4.42×10^{-4}	7.96×10^{-6}	18	27	666
		0.32					16	301
		1.6					3.5	56
	0.006	0.16					27	666
		0.32					15	299
		1.6					3.4	56
2b	0.012	0.16	2.76×10^{-2}	1.64×10^{-4}	1.03×10^{-5}	168	4.1	163
		0.32					2.0	80
		1.6					0.40	16
2c	0.024	0.16	1.16×10^{-2}	1.01×10^{-3}	9.45×10^{-6}	12	38	559
		0.32					23	220
		1.6					5.3	38
	0.012	0.16					37	536
		0.32					22	217
		1.6					5.2	38
	0.006	0.16					36	526
		0.32					22	215
		1.6					5.2	38
2d	0.012	0.16	2.59×10^{-2}	1.65×10^{-3}	2.19×10^{-5}	16	30	214
		0.32					17	93
		1.6					3.9	17

[a]Values determined at stoichiometric catalyst concentrations, at 25 ºC in $Et_3N/Et_3NH^+Cl^-$ buffer, from our previously reported data[S4].[b]k_1 refers to the adduct (**III**) forming step from catalyst (**I**) and benzaldehyde.[c]k_{-1} refers to adduct (**III**) dissociation into catalyst (**I**) and benzaldehyde. [d]Values obtained from use of previous data[S4] at stoichiometric catalyst concentrations, as described in section S3.[e]K_1 refers to the equilibrium constant for adduct (**III**) from catalyst (**I**) and benzaldehyde.[f]Determined through use of rate constants in Berkeley-Madonna equation solver for a chemical reaction profile. [g]Values from the Equation S. 1 for half life in forward direction to adduct formation summarised above using the rate constants summarised herein.

S5 Hammett Plot including Data for Triazolium Salt 2f

Datapoints using literature σ values for the N-pentafluorophenyl substituent of catalyst **2f** are highlighted in the plot below with σ values obtained from refs. S9-11. Irrespective of the σ value used, the data point for **2f** deviates significantly below the correlation line obtained using data for para-substituted triazolium catalysts only. Of the literature σ values, that from Chang *et al.* yielded the closest correlation. This value was obtained from correlating a selection of pK_a values of pentafluorophenyl-substituted alcohols to the standard correlation equation for non-fluorinated alcohols, for which pentafluorophenyl derivatives deviate significantly. The value of 1.96 by Brink *et al*. was obtained from the pK_a value of pentafluorophenyl carboxylic acid. Finally, the value of 1.5 by Korenaga *et al.* was obtained from correlating the carbonyl stretching frequency of a selection of substituted esters. This final method has the advantage of not relying on a potentiometric titration unlike the previous two estimates. Potentiometric titration of pentafluorophenyl-derived species is described as unsuitable due to the instability of the pentafluorophenyl moiety with respect to oxyanions at the *para*-position.[S9-S11]

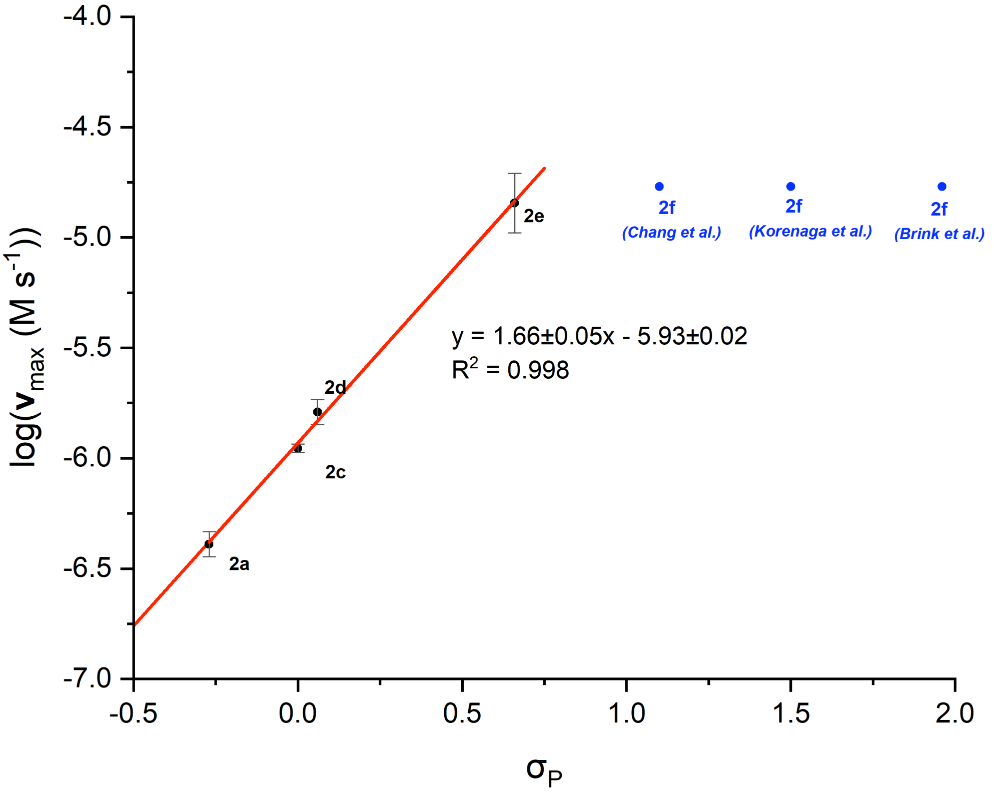

*Figure S. 23. Hammett plot for para-substituted triazolium salts **2a** and **2c-2e** (data points in black) with data for **2f** (in blue) included using the three reported literature Hammett σ-values for a pentafluorophenyl substituent; these data for **2f** were not included in determining the slope of the correlation.*

S6 ‘Brønsted’ Plots

A Brønsted-type plot was constructed by plotting log(k_{BI}/[**I**]) versus published pK_a values for the triazolium catalysts **2a-f** in water and DMSO from previous studies by ourselves[S6], Cheng[S7] and Harper[S8]. Although not a true Brønsted plot, which by definition should utilise adduct C(α)-H pK_a values, the Brønsted-α values of 1.71 in water and 0.65 in DMSO show a clear dependence on the acidity of catalyst with higher k_{BI} values observed for catalysts with lower pK_a values. The correlation with aqueous pK_a values is more appropriate for comparison with our present study in a protic solvent methanol. Electron withdrawing N-aryl substituents are observed to decrease triazolium pK_a (increase acidity)[S6-S8] and a similar N-Ar substituent dependence is observed for v_{max} (and k_{BI} as assumed herein) supporting proton transfer as a likely rate-determining step.

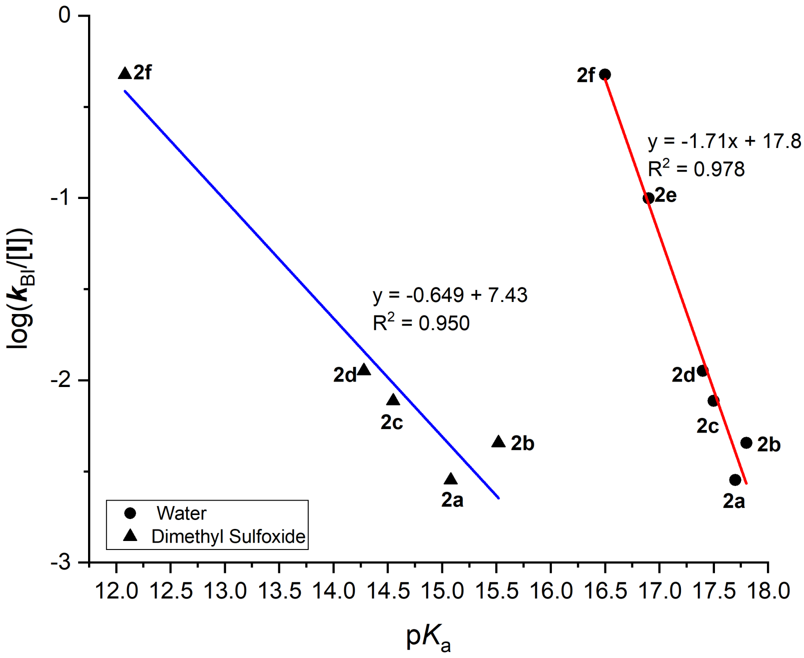

*Figure S.24: ‘Brønsted’ type plots for catalysts **2a-f** in DMSO and H_2O.* pK_a values in H_2O and DMSO were taken from references S4 and S5-S6, respectively.[S6-S8]

S7 HPLC Chromatograms of Benzoin versus Benzaldehyde

Benzaldehyde and benzoin are both commercially available and were used to obtain the reference HPLC traces shown below. Throughout the studies it was seen that the benzaldehyde peak decreased whilst the benzoin peak grew. The benzoin condensation has been studied extensively by other techniques, including ^{1}H NMR spectroscopy, in our previous work (*e.g.* refs. S4 and S5).

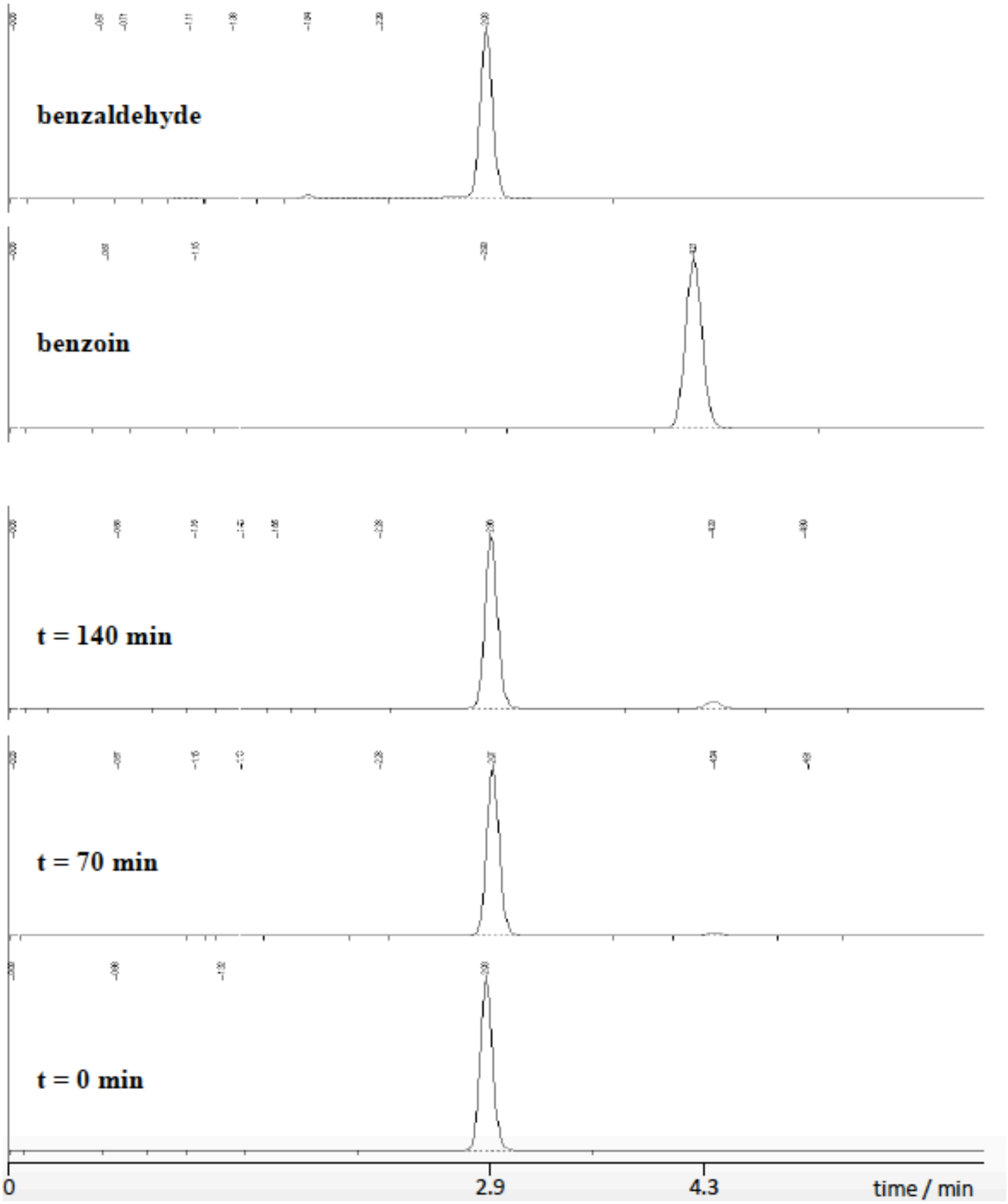

*Figure S. 25. HPLC traces for commercial benzaldehyde and benzoin, and a representative kinetic experiment showing progress of the benzoin condensation of benzaldehyde (0.64 M) catalysed by thiazolium salt **1** (12 mM) at 50 °C in triethylamine-buffered methanol at t= 0, 70 and 140 min demonstrating growth of benzoin peak over time.*

S8 References

S1. H. E. Gottlieb, V. Kotlyar and A. Nudelman, *J. Org. Chem.*, 1997, **62**, 7512-7515.

S2. M. S. Kerr, J. Read de Alaniz and T. Rovis, *J. Org. Chem.*, 2005, **70**, 5725-5728.

S3. K. B. Ling and A. D. Smith, *Chem. Commun.*, 2011, **47**, 373-375.

S4. C. J. Collett, R. S. Massey, J. E. Taylor, O. R. Maguire, A. C. O'Donoghue and A. D. Smith, *Angew. Chem. Int. Ed.*, 2015, **54**, 6887-6892.

S5. C. J. Collett, R. S. Massey, O. R. Maguire, A. S. Batsanov, A. C. O'Donoghue and A. D. Smith, *Chem. Sci.*, 2013, **4**.

S6. R. S. Massey, C. J. Collett, A. G. Lindsay, A. D. Smith and A. C. O'Donoghue, *J. Am. Chem. Soc.*, 2012, **134**, 20421-20432.

S7. Z. Li, X. Li and J. P. Cheng, *J. Org. Chem.*, 2017, **82**, 9675-9681.

S8. N. Konstandaras, M. H. Dunn, M. S. Guerry, C. D. Barnett, M. L. Cole and J. B. Harper, *Org. Biomol. Chem.*, 2020, **18**, 66-75.

S9. T. Korenaga, K. Kadowaki, T. Ema and T. Sakai, *J. Org. Chem.*, 2004, **69**, 7340-7343.

S10. I. S. Chang, J. T. Price, A. J. Tomlinson, C. J. Willis, *Can. J. Chem.*, 1972, **50**, 512-520.

S11. H. Brink, *Acta Pharm. Suec.,* 1980, **17**, 233-248.